

Reliability analysis of very slender columns subjected to creep

Kleyser Ribeiro^{a*} , Daniel Domingues Loriggio^a , Mauro de Vasconcellos Real^b 

^a Universidade Federal de Santa Catarina - UFSC, Florianópolis, Santa Catarina, Brasil. E-mail: kleyser.ribeiro@gmail.com, d.loriggio@gmail.com

^b Universidade Federal do Rio Grande - FURG, Rio Grande, Rio Grande do Sul, Brasil. E-mail: mvrealgm@gmail.com

* Corresponding author

<https://doi.org/10.1590/1679-78256569>

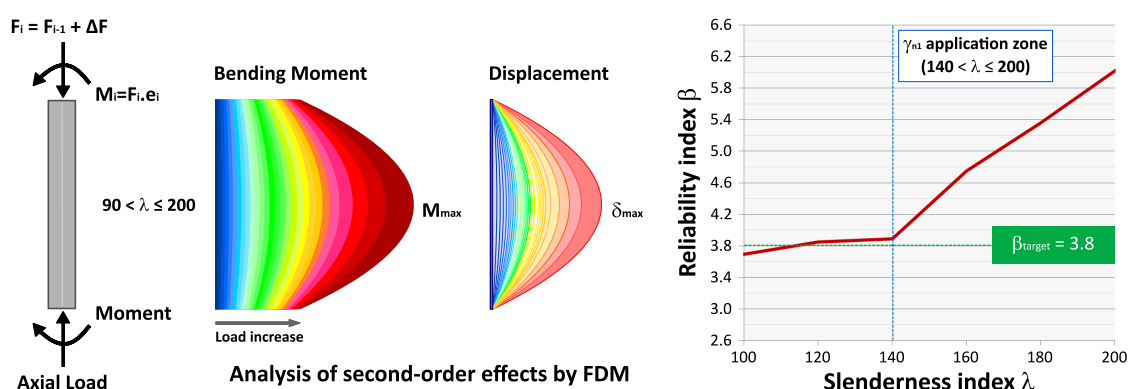
Abstract

A mechanical model was developed to evaluate the reliability of very slender columns subject to creep, employing the nonlinear moment-curvature relationship. Second-order effects were considered by the finite difference method. Numerical tests were carried out on 432 columns with a slenderness index between 100 and 200. The general nonlinear method was adopted to determine the design load, applying the displacement of the stress-strain diagram for consideration of creep. The reliability index was calculated using the Monte Carlo method and the First Order Reliability Method. Among the results obtained, it was observed that it is important to review the safety criterion of the Brazilian Standard NBR 6118 about the very slender columns ($90 < \lambda \leq 200$) by performing the calibration of the additional coefficient γ_{n1} . In addition, it was observed that an increase in the reinforcement ratio commonly produces a reduction in the reliability index; an increase in the first-order relative eccentricity promotes a decrease in reliability, among other evaluated factors.

Keywords

Slender columns; Structural reliability; Moment-curvature; Second-order effects; Creep.

Graphical Abstract



Received May 21, 2021. In revised form September 12, 2021. Accepted September 12, 2021. Available online September 17, 2021.

<https://doi.org/10.1590/1679-78256569>



Latin American Journal of Solids and Structures. ISSN 1679-7825. Copyright © 2021. This is an Open Access article distributed under the terms of the [Creative Commons Attribution License](https://creativecommons.org/licenses/by/4.0/), which permits unrestricted use, distribution, and reproduction in any medium, provided the original work is properly cited.

1 INTRODUCTION

Considering that Brazil presents a favorable condition about the absence of seismic activity and other natural phenomena, it is possible to construct slender buildings. In this way, more slender columns also are observed, in which the second-order effects become quite significant. The Brazilian Standard NBR 6118 (ABNT, 2014) admits the design of columns with a slenderness index (λ) up to 200. However, there are few studies on the behavior of elements with $\lambda > 90$, since above this level of slenderness it is required the application of laborious numerical methods. Furthermore, creep effects should be considered in columns with $\lambda > 90$ and only the general method can be used for elements with $\lambda > 140$, with an additional coefficient γ_{n1} being required for $140 < \lambda \leq 200$. Therefore, several requirements related to very slender columns need to be analyzed to guarantee the reliability of this type of structural element.

Given this condition, an analysis was made of the structural reliability of columns with a slenderness index between 100 and 200, based on the Brazilian Standard for reinforced concrete. About 432 elements with square or rectangular cross-section were considered, varying the following parameters: cross-section dimensions, slenderness index (λ), characteristic compressive strength of concrete (f_{ck}), first-order relative eccentricity (e_1/h) and reinforcement ratio (ρ). The general nonlinear method was applied in all cases, considering the creep effects through the effective creep coefficient (φ_{ef}) with the displacement of the stress-strain diagram, based on Fusco (1981) and Casagrande (2016). The curvature ($1/r$) of each section was obtained from the moment-curvature relationship ($M-1/r$), and the second-order effects were determined using the finite difference method (FDM). To determine the reliability index (β) and the probability of failure (P_f), the Monte Carlo method and First Order Reliability Method (FORM) were used.

Researchers from other countries have also studied second-order effects in very slender columns, as can be seen in Strauss et al. (2018) and Benko et al. (2019). However, in these studies, the emphasis was placed on Eurocode 2 (CEN, 2004) using the global safety factor. Therefore, the reliability index and the respective probability of failure have not been determined. Several studies were limited to second-order effects on columns with $\lambda < 90$, such as: Damas (2015), Magalhães et al. (2016), Barbosa (2017) and Klein Júnior et al. (2020). Thus, there is a vast field of research to be explored, aiming to meet the demand of contemporary engineering in the face of advances in the technology of design tools, materials, and building systems.

This research was limited to reinforced concrete elements subjected to compression load with a uniaxial moment. It was intended to evaluate the reliability of very slender columns using the general nonlinear method and the linear creep theory. Therefore, the following items were analyzed: reliability index (β) in relation to the target reliability index (β_t); adequacy of the additional coefficient γ_{n1} with regard to its range of application and its results; variation of the reliability index in function of the variation of the dimensions of the cross-section; and influence of the other parameters considered in the value of the reliability index. In this way, it was possible to evaluate the recommendations of the Brazilian Standard for columns with $90 < \lambda \leq 200$ and check if there is a need for adjustments.

2 DESIGN MODEL

According to the Brazilian Standard NBR 6118 (ABNT, 2014), for columns with slenderness index λ above 90, the following methods are allowed: model column method coupled to M-N-1/r diagrams, which is an approximate process for elements with $\lambda \leq 140$; and general nonlinear method, with the application of the moment-curvature relationship and use of a non-approximate process to consider second-order effects. A linearization of the moment-curvature diagram characterized by the secant stiffness can be used to calculate deformations. The two possibilities for considering the moment-curvature relationship are shown in Figure 1. It should be noted that the application of the safety formulation in which the second-order effects of the increased loads of γ_f / γ_{f3} are calculated to be later increased by $\gamma_{f3} = 1.1$, is permitted by the Brazilian Standard, but it is not mandatory.

It is emphasized that only the nonlinear moment-curvature diagram was used throughout this work. The dimensionless curvature (θ) was adopted, depending on the overall cross-section depth (h) and the curvature ($1/r$), according to Equation 1.

$$\theta = 1000 h \frac{1}{r} \quad (1)$$

For the computational implementation of the moment-curvature relationship for the design condition, the algorithm shown in Figure 2 was adopted. From the flowchart, it is observed that there are several necessary checks. For example, in determining the curve corresponding to $0.85 f_{cd}$, the strains in the section should be checked about the

ultimate strains of the materials, obtaining the ultimate moment (M_{Rd}). In turn, the curve for $1.10 f_{cd}$ should be limited to the ultimate moment calculated by the previous curve.

Material properties were included through constitutive relationships. For concrete, the simplified parabolic-rectangle diagram was adopted. Creep was considered by displacing this diagram with the application of the effective creep coefficient φ_{ef} , based on Fusco (1981) and Casagrande (2016).

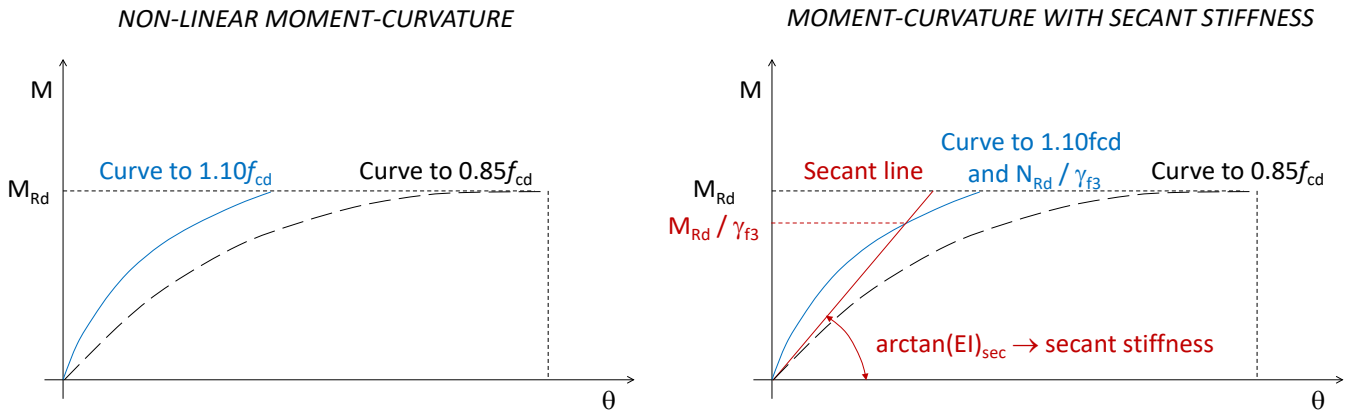


Figure 1 Options for applying the moment-curvature relationship.

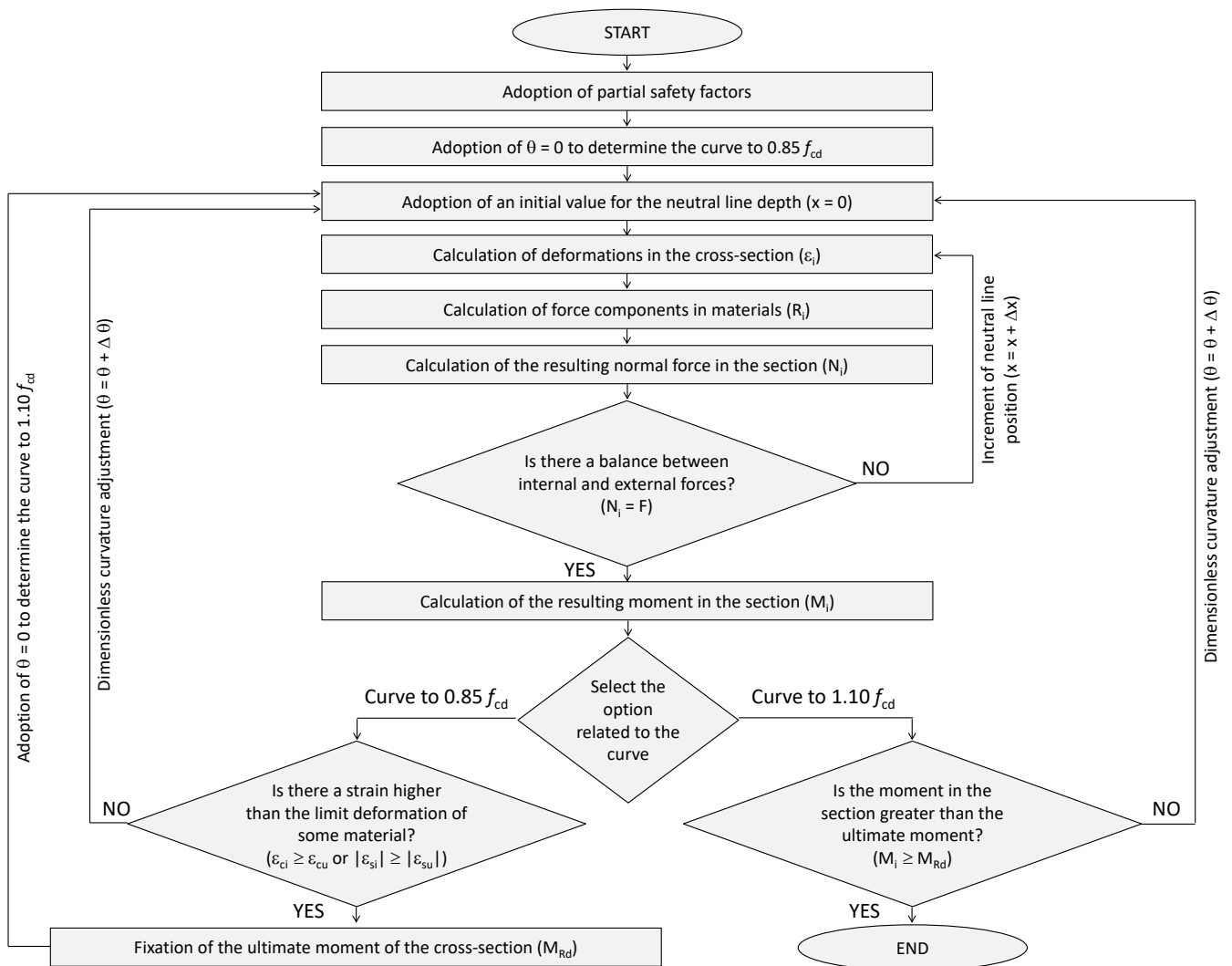


Figure 2 Flowchart to implement the moment-curvature relationship for the design condition.

The proportion of 75% of the long-term load was admitted, resulting in $\phi_{ef} = 1.18$. The Brazilian Standard NBR 6118 (ABNT, 2014) also considers creep approximately, including an additional eccentricity e_{cc} . However, this will not be seen in this paper, as a more precise procedure is adopted. The tensile stresses in the concrete were neglected in the design procedures, as their consideration is not allowed in the design model of the Brazilian Standard. For the steel of the longitudinal reinforcement, the perfect elasto-plastic behavior was considered valid for both tension and compression. The stress-strain diagrams are shown in Figure 3.

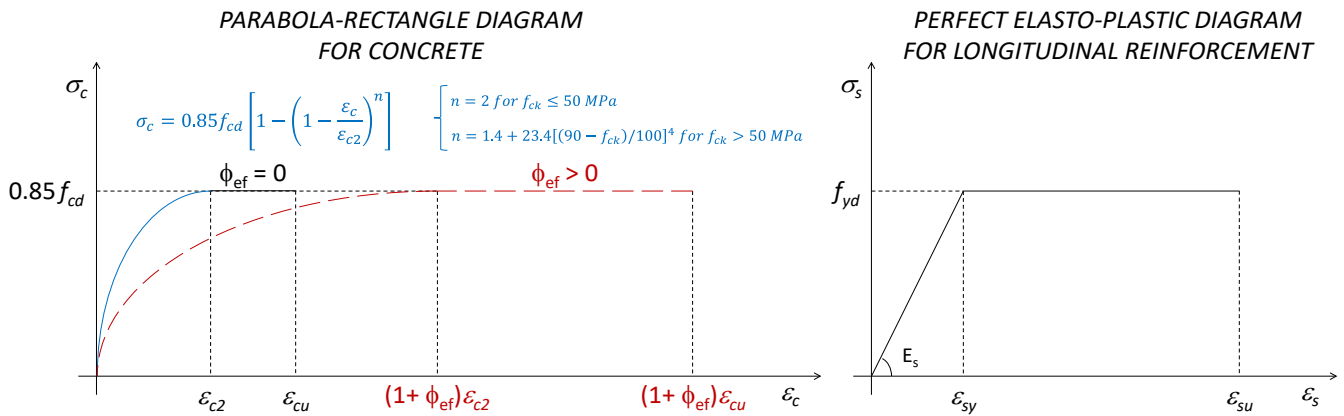


Figure 3 Stress-strain diagrams for concrete and longitudinal reinforcement (design model).

The moment-curvature relationship contemplates physical nonlinearity, considering the materials that make up the cross-section working together. However, it is also necessary to consider geometric nonlinearity when calculating very slender columns. Therefore, it is needed to select a non-approximate calculation procedure that evaluates the displacements in the axis of the element to determine the bending moments and verify the stability. This verification is essential, given the risk relative to the loss of stability of the very slender columns.

In Figure 4, the bending moment diagrams are presented for a column subjected to an increasing axial load ($F_i = F_{i-1} + \Delta F$), as in an experimental test. The moment (M_i) is the result of the product between the applied force (F_i) and the eccentricity (e_i) in relation to the axis of the element. As the load increases, the displacement of the axis also increases ($\delta_i = \delta_{i-1} + \Delta \delta$). This generates ever-greater bending moments until the rupture of the cross-section or loss of stability of the column. In this study, the finite difference method (FDM) was selected to determine second-order effects.

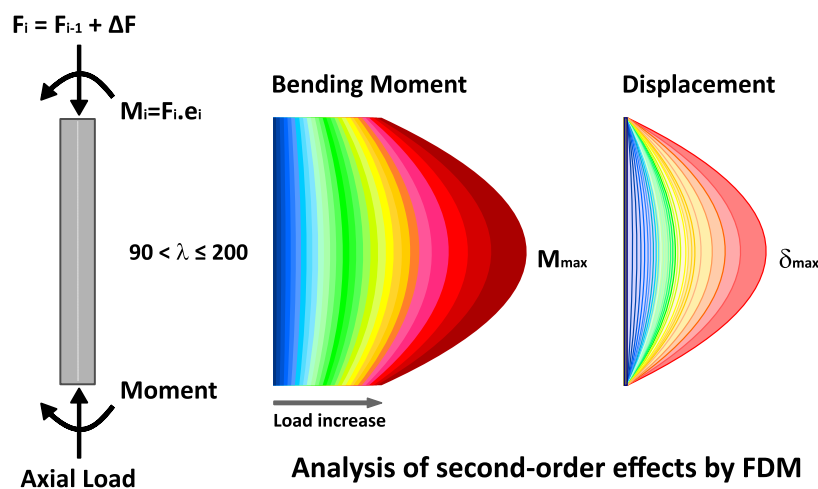


Figure 4 Load increment process and its moment and displacement results.

Seeking to elucidate the process of applying the finite difference method (FDM) to the reinforced concrete columns, the computational implementation algorithm is shown in Figure 5. The cantilever column equivalent to the pinned-pinned column was used to calculate the displacements to reduce computational effort.

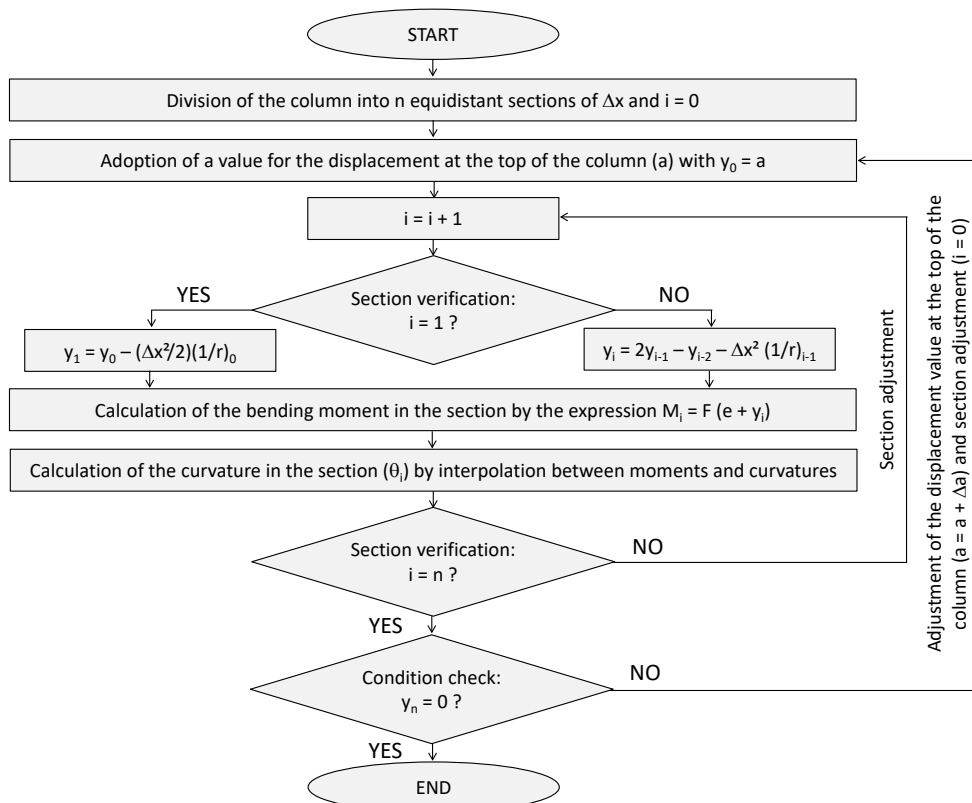


Figure 5 Flowchart to implement the finite difference method.

Besides, for columns with $\lambda > 140$, the Brazilian Standard NBR 6118 (ABNT, 2014) requires an additional coefficient γ_{n1} in the analysis of second-order effects, given by Equation 2, which should multiply the design loads.

$$\gamma_{n1} = 1 + [0.01 (\lambda - 140)/1.4] \tag{2}$$

3 MECHANICAL MODEL

The resistance of the columns should be determined based on experimental tests. However, they are laborious and expensive. In probabilistic analysis, numerical methods are applied to estimate such values. Thus, it is common to develop a mechanical model to represent the behavior of the elements. This model differs from the design model due to its distinct characteristics. In other words, a computational model is elaborated, which must be validated from the experimental results. To develop a suitable mechanical model, it is necessary to adapt the general nonlinear method. First, all safety factors must be disregarded. Then, a moment-curvature relationship with a single curve is applied for the mean value of concrete compressive strength (f_{cm}), as shown in Figure 6.

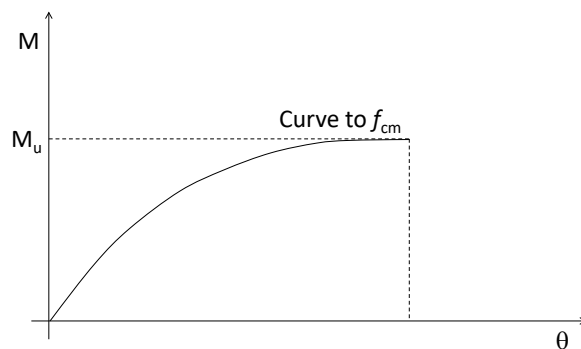


Figure 6 Moment-curvature relationship for the mechanical model.

Searching for a computational model with more reliable behavior in relation to physical models, the stress-strain relationship of nonlinear analysis was used for the concrete subjected to compression, according to Eurocode 2 (CEN, 2004). Concrete tensile strength was also considered, including the tension stiffening effect, according to Collins & Mitchell (1997). Both cases are shown in Figure 7. The displacement of the concrete diagrams is considered due to the creep effect through the effective creep coefficient ϕ_{ef} . In the case of tension, there is also a drop due to the coefficient α_2 , when the element is subjected to the sustained load. The perfect elasto-plastic behavior was considered for longitudinal reinforcement, as seen in Figure 3, but with no safety factor.

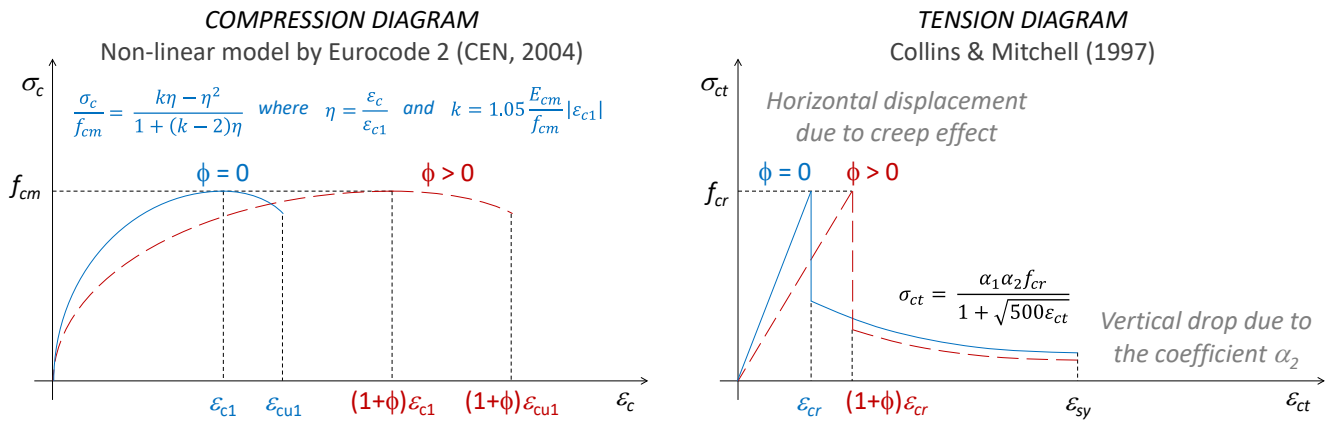


Figure 7 Concrete stress-strain diagrams for the mechanical model.

Considering that safety factors should not be adopted in the mechanical model, the algorithm for determining the moment-curvature relationship is shown in Figure 8.

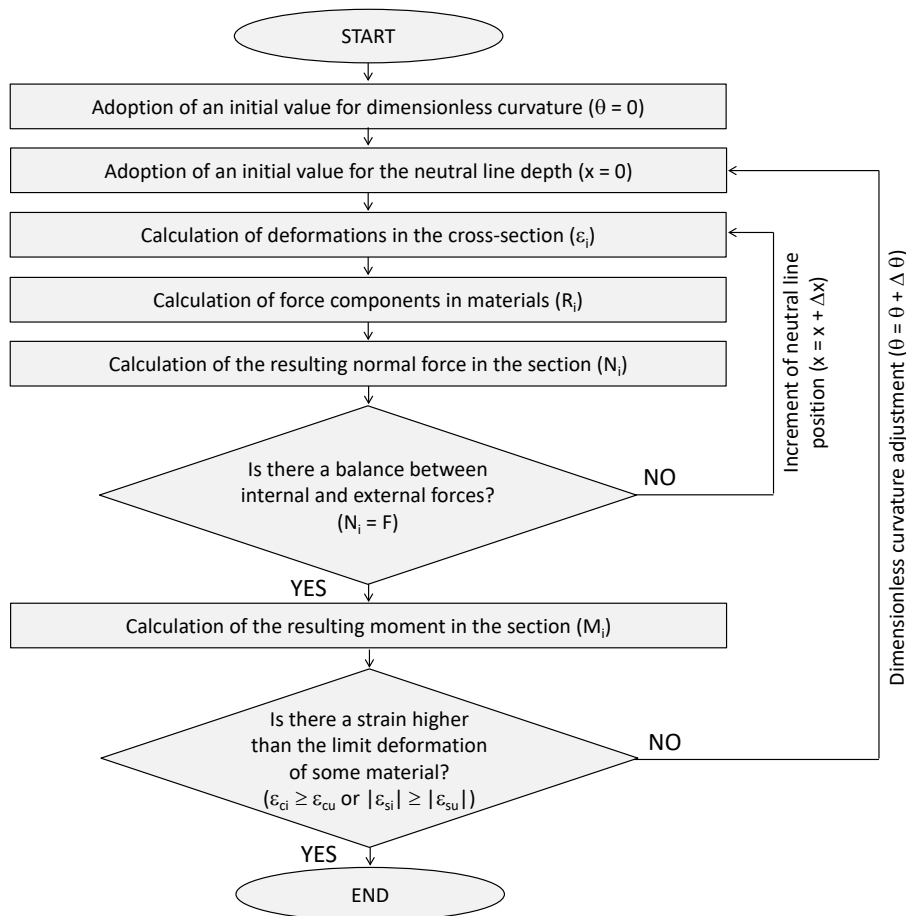


Figure 8 Flowchart to implement the moment-curvature relationship for the mechanical model.

As previously mentioned, the mechanical model needs to be validated based on experimental results. For this reason, a database was developed based on results available in the literature obtained by several authors, considering slender columns subjected to short-term and sustained loadings. The main characteristics of the columns subjected to short-term loading are presented in Table 1. The characteristics of the elements tested for sustained loading are shown in Table 2, which were also evaluated in Westerberg (2008).

Table 1 Database with short-term loading columns considered in the model validation.

Reference	Number of columns	Dimensions of the cross-section (b x h) in mm	Distribution of steel bars (see Figure 9)	f_c (MPa)	ρ (%)	λ	e_1/h
Claeson & Gylltoft (1998)	12	120x120 or 200x200	(A)	33.0 to 93.0	1.99 to 3.11	52 to 69	0.10 to 0.17
Dantas (2006)	5	250x120	(B)	33.9 to 37.6	1.57	87	0.12 to 0.50
Enciso (2010)	4	250x150	(A), (B), (C)	46.9 to 53.6	1.26 to 4.29	69	0.13
Goyal & Jackson (1971)	26	76.2x76.2	(A)	19.9 to 23.6	1.72 to 2.45	55 to 125	0.17 to 0.50
Kim & Lee (2000)	4	100x100 or 200x100	(A), (B)	27.0	2.13 to 2.84	42	0.40
Kim & Yang (1995)	18	80x80	(A), (D)	25.5 to 86.2	1.98 to 3.95	62 to 104	0.30
Melo (2009)	17	250x120	(B)	37.2 to 45.8	1.57	58 to 87	0.05 to 0.50

Table 2 Database with sustained loading columns considered in the model validation.

Reference	Number of columns	Dimensions of the cross-section (b x h) in mm	Distribution of steel bars (see Figure 9)	f_c (MPa)	ρ (%)	λ	e_1/h
Goyal & Jackson (1971)	20	76.2x76.2	(A)	19.9 to 23.6	1.72 to 2.45	55 to 125	0.17 to 0.50
Khalil et al. (2001)	8	b = 152 80 ≤ h ≤ 125	(A)	41.5 to 53.6	2.58 to 4.23	100 to 216	0.08 to 0.12
Kordina (1972)	10	264 ≤ b ≤ 272 172 ≤ h ≤ 176	(A)	20.9 to 27.1	0.98 to 3.19	101 to 104	0.20 to 0.50
Ramu et al. (1969)	8	250x150	(C)	21.5 to 37.2	1.66 to 4.21	100	0.03 to 0.25

Altogether, 132 columns were evaluated in the database. There are 46 columns subjected to long-term loading, for which the value of the effective creep coefficient must be calculated. For short-term loading, it is assumed that there is no creep effect. The cross-section is square or rectangular in all cases, defined by the width (b) and the overall depth (h). The distribution of the longitudinal reinforcement bars is shown in Figure 9, where the support scheme is also observed.

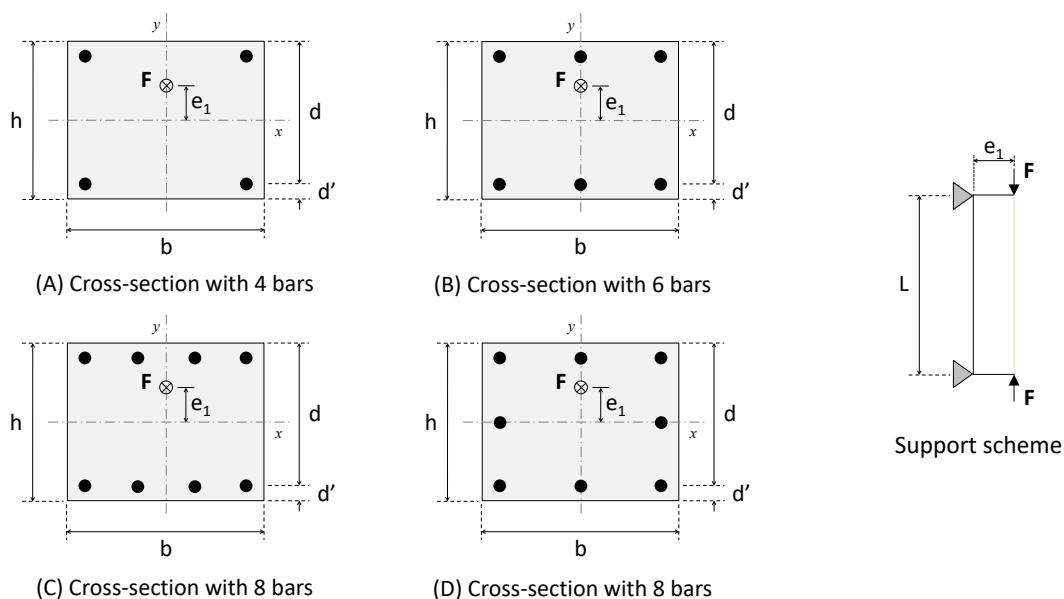


Figure 9 Cross-sections and support scheme of the columns considered in the database.

Graphs were drawn up for some relevant characteristics. First, the columns were divided into two groups, according to the type of loading they are subjected to, short or long-term. Then, their distribution concerning the slenderness index was demonstrated. In addition, the distribution of the values considered for the effective creep coefficient of the columns subjected to the sustained loading is presented, as shown in Figure 10.

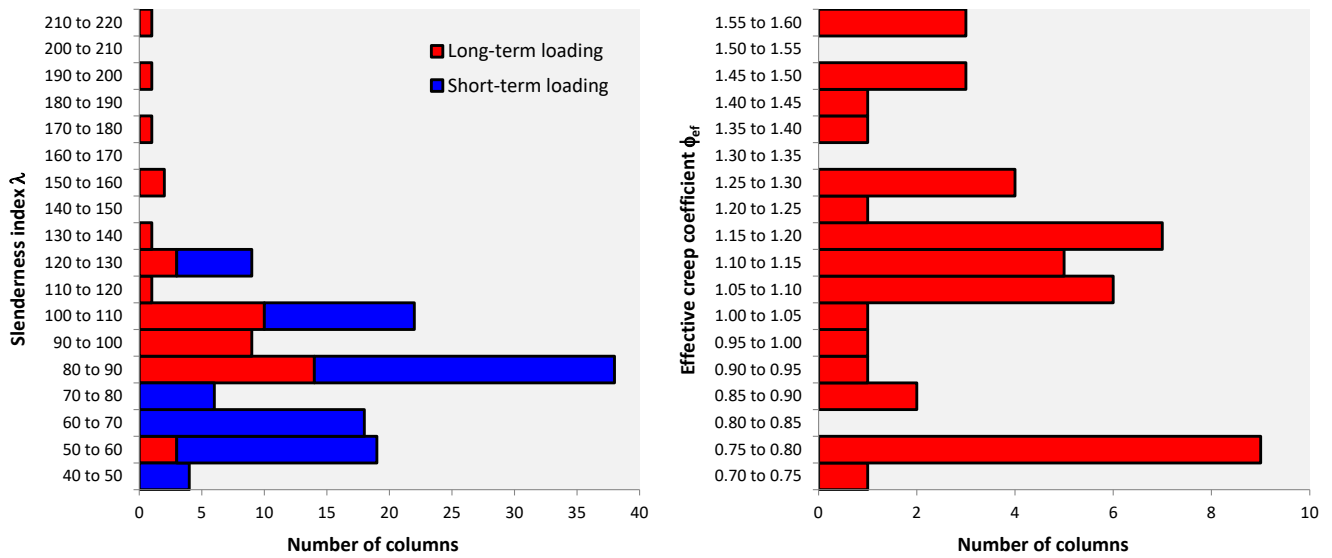


Figure 10 Distribution of columns in the database according to the slenderness index and effective creep coefficient.

Using the developed computer program, numerical tests were performed for all columns presented in Tables 1 and 2. The results of the mechanical model (F_{mod}) showed good adherence to the experimental results (F_{exp}), as can be seen in Figure 11. In addition, the range of variation of the values found for the F_{exp} / F_{mod} ratio is demonstrated, identifying the mean and extreme values.

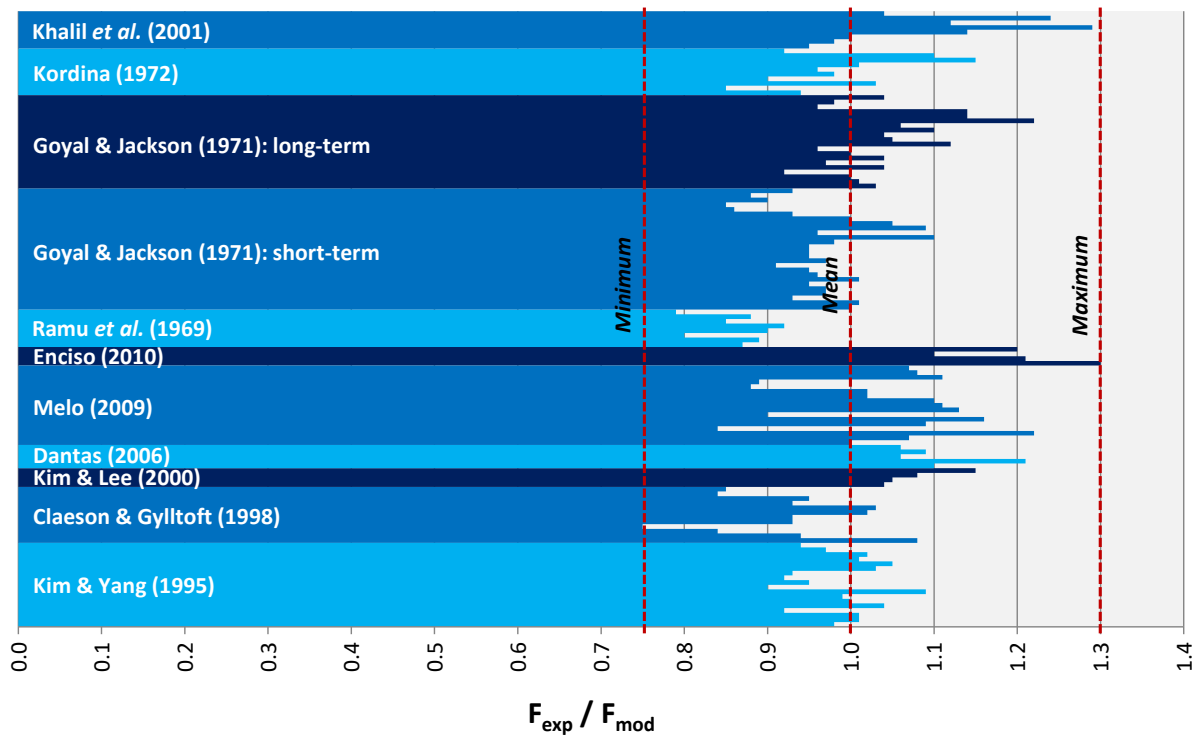


Figure 11 F_{exp} / F_{mod} ratio for all columns analyzed in the model validation.

The statistical parameters presented in Table 3 were obtained based on the database, considering the ratio between the ultimate experimental load F_{exp} and the ultimate model load F_{mod} . It is observed that the mechanical model fits well with the experimental results, given the mean value $\mu = 1.00$ and the standard deviation $\sigma = 0.10$. It should be noted that the data dispersion was small, given the minimum of 0.75 and maximum of 1.30 obtained for the quotient.

Table 3 Statistical synthesis of results based on the F_{exp} / F_{mod} ratio.

Minimum	Maximum	Range	Mean (μ)	Standard deviation (σ)	Coefficient of variation (COV)
0.75	1.30	0.55	1.00	0.10	0.10

One cannot fail to consider the variation of the computational model results through the model error e_{model} , according to Mirza & Skrabek (1991). Its value is obtained by Equation 3, where $\mu_{model} = 1.00$ and z is a Gaussian random variable with zero mean and standard deviation equal to one. V_{model} is the coefficient of variation of column strength due to inaccuracies in the theoretical model. Therefore, it is important to apply this correction method to the ultimate load values obtained by the mechanical model.

$$e_{model} = \mu_{model}(1 + z \cdot V_{model}) \quad (3)$$

The value of V_{model} is given by Equation 4, where $V_{t/c}$ is the coefficient of variation of the ratio of test to computed strengths (admitted equal to COV of F_{exp} / F_{mod}), $V_{in-batch}$ is the coefficient of variation of column strength due to in-batch variabilities of all variables affecting its strength, and V_{test} is the coefficient of variation of column strength due to testing procedures. After the relevant calculations and considerations, it is assumed that $V_{t/c} = 0.10$, $V_{in-batch} = 0.044$ and $V_{test} = 0.04$.

$$V_{model} = \sqrt{V_{t/c}^2 - V_{in-batch}^2 - V_{test}^2} \quad (4)$$

Such data result in $V_{model} = 0.08$ for the mechanical model developed in this work. Thus, it is considered that it is suitable for performing numerical tests.

4 STRUCTURAL RELIABILITY

To evaluate the reliability of structures, it is necessary to determine their *limit state function*, according to Equation 5, where the resistance (R) and the load effect (S) are considered. The resistance is obtained from the product between the ultimate load ($F_{u, mod}$) and the model error (e_{model}). The other part gives the load effect by the sum of permanent and variable loads, F_g and F_q , respectively.

$$g(R, S) = R - S = e_{mod}F_{u, mod} - (F_g + F_q) \quad (5)$$

As seen earlier, the resistance value comes from the mechanical model, and the load effect value comes from the design model. According to Nowak & Collins (2000), the safety margin $g(R, S)$ is obtained from the difference between R and S . Thus, it is necessary to identify the appropriate probability density function (PDF) for each variable. Frequently, the normal distribution is adopted for both. However, its adherence to the data must be verified utilizing a normality test. In turn, the probability of failure (P_f) can be calculated from Equation 6.

$$P_f = P(R - S < 0) = P(g < 0) \quad (6)$$

The relationship between the probability density functions (PDF) for resistance (R) and load effect (S) must be evaluated, according to Figure 12, adapted from Nowak & Collins (2000). The occurrence of a failure zone is observed when there is an overlap between the two curves. Consequently, a probability of failure (P_f) is observed regarding the negative values that appear for the curve referring to the safety margin (g).

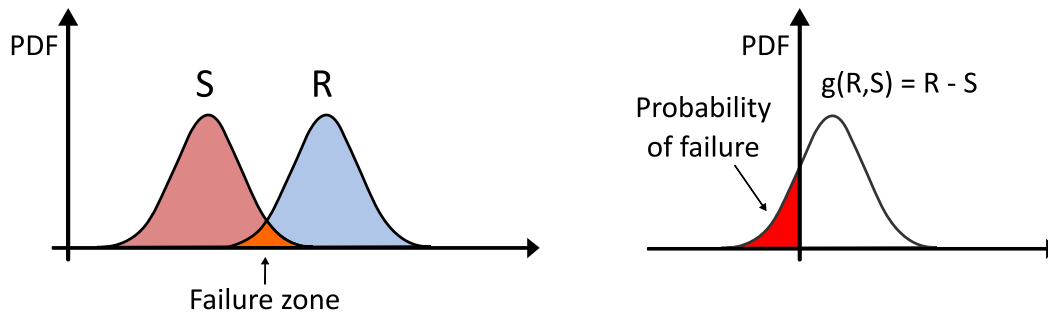


Figure 12 Relationship between resistance and load effect, adapted from Nowak & Collins (2000).

For the parametric analysis, random variables were adopted, with their respective probability distribution, as shown in Table 4. In most cases, the variables considered fit well with the normal distribution, except for the variable load (F_q), which has greater adherence to the distribution of Gumbel's extreme value I. Another significant observation concerns variability. The variable load has the highest coefficient of variation (COV) among all the variables considered. Therefore, its intensity can have a significant influence on the value of the reliability index.

Table 4 Random variables considered in the parametric analysis.

Random variable	Distribution	Mean (μ)	Standard deviation (σ)	References
Compressive strength of concrete (f_c)	Normal	$\mu_{f_c} = \frac{f_{ck}}{1 - 1.645 V_{f_c}}$ where $V_{f_c} = 0.10$	$\sigma_{f_c} = \mu_{f_c} V_{f_c}$ where $V_{f_c} = 0.10$	Magalhães (2014) Damas (2015) Barbosa (2017)
Yield strength of reinforcement (f_y)	Normal	$\mu_{f_y} = 1.09 f_{yk}$	$\sigma_{f_y} = 0.05 \mu_{f_y}$	Damas (2015)
Width of the cross-section (b)	Normal	$\mu_b = b$ (nominal design value)	$\sigma_b = 0.5$ cm	Nogueira (2006) Magalhães (2014) Damas (2015) Barbosa (2017)
Overall depth of the cross-section (h)	Normal	$\mu_h = h$ (nominal design value)	$\sigma_h = 0.5$ cm	Nogueira (2006) Magalhães (2014) Damas (2015) Barbosa (2017)
Effective depth of the cross-section (d)	Normal	$\mu_d = d$ (nominal design value)	$\sigma_d = 0.5$ cm	Magalhães (2014) Damas (2015) Barbosa (2017)
Permanent load (F_g)	Normal	$\mu_{F_g} = 1.05 F_{gk}$	$\sigma_{F_g} = 0.10 \mu_{F_g}$	Nogueira (2006) Magalhães (2014) Damas (2015)
Variable load (F_q)	Gumbel's extreme value I	$\mu_{F_q} = F_{qk}$ (characteristic value)	$\sigma_{F_q} = 0.25 \mu_{F_q}$	Nogueira (2006) Magalhães (2014) Damas (2015)

In Santiago et al. (2020), some statistics related to Brazilian reality are presented. Based on more than 39 thousand cylindrical concrete specimens made in Brazil and submitted to the axial compression test, the mean and the COV decrease with the increase of the characteristic compressive strength. However, the average values are close to the results found by the formulation proposed by Magalhães (2014), Damas (2015), and Barbosa (2017). Therefore, the use of the relationship seen in Table 4 is justified. For the other random variables, greater variability was observed in some experimental tests. However, the observed variation does not compromise the validity of the adopted propositions based on the literature.

The Monte Carlo method was applied to obtain 500 simulations, according to the flowchart shown in Figure 13. It is noteworthy that the determination of the number of simulations was adequately analyzed since the process has a good convergence to it. Furthermore, the same sample size was also evaluated by other researchers, such as Damas (2015), Magalhães et al. (2016), and Barbosa (2017). However, the value of the reliability index (β) was calculated from the First Order Reliability Method (FORM), adopting the algorithm proposed by Magalhães (2014), according to the flowchart shown in Figure 14.

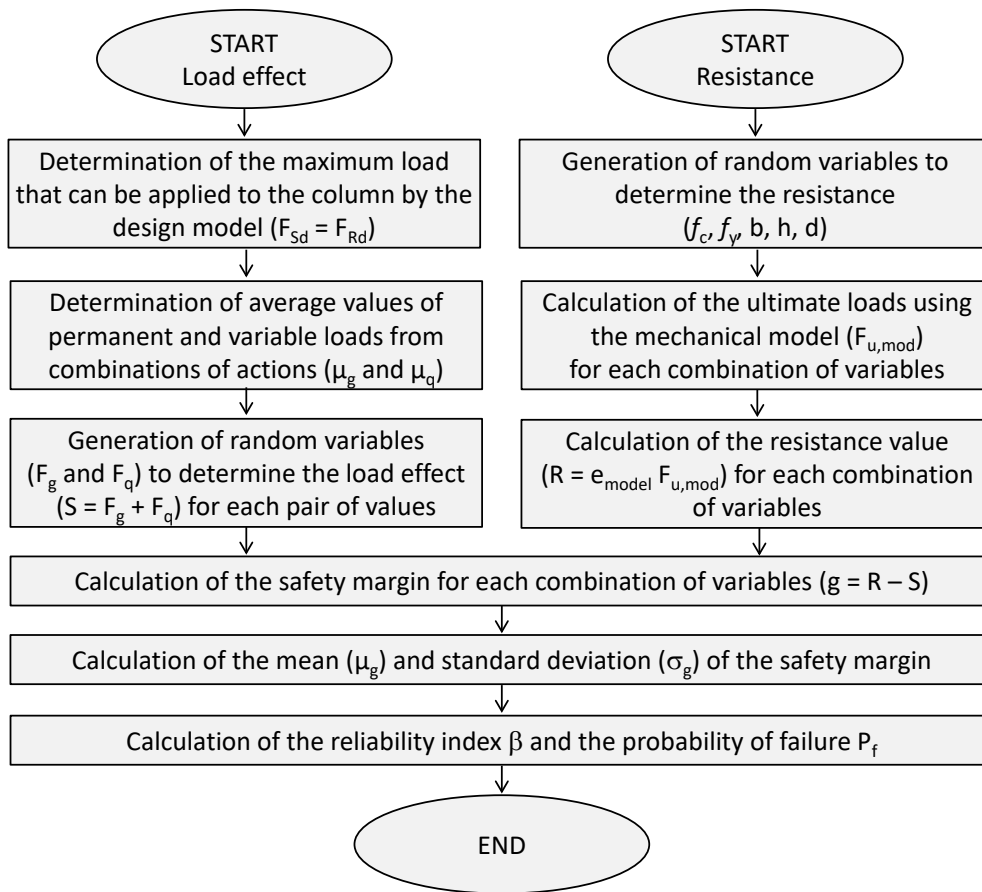


Figure 13 Flowchart of application of the Monte Carlo method.

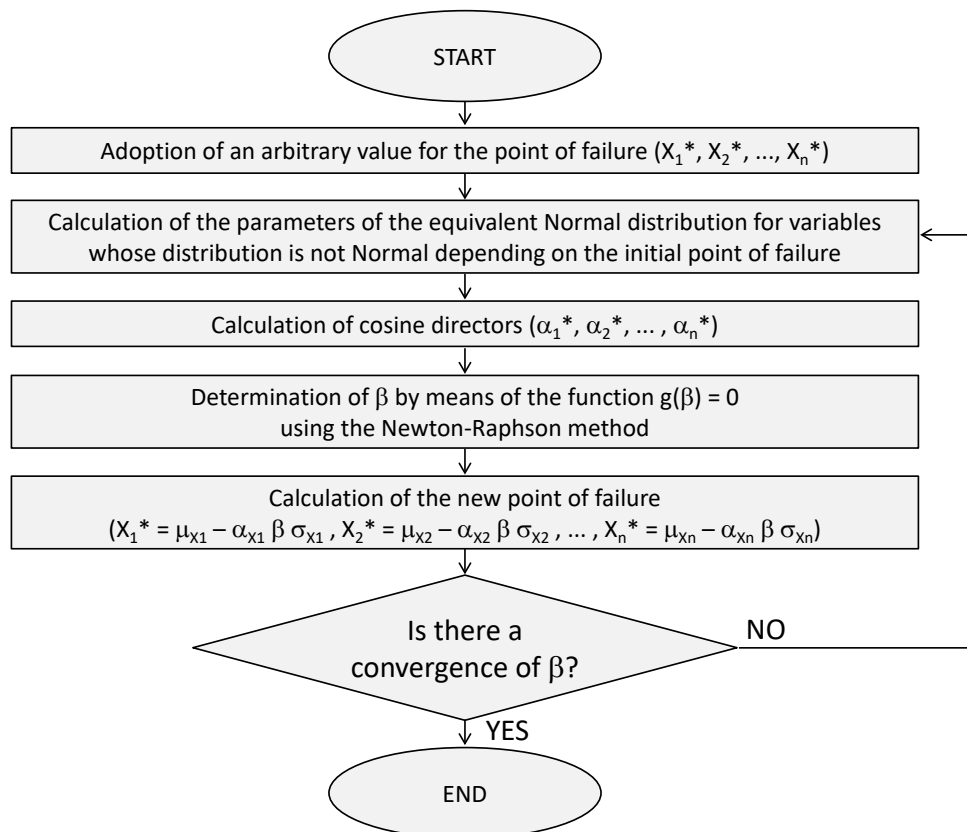


Figure 14 Flowchart of application of the FORM based on Magalhães (2014).

5 NUMERICAL TESTS

Numerical tests were performed on 432 columns with a slenderness index between 100 and 200. Square and rectangular cross-sections were adopted, as shown in Figure 15. The variation in dimensions was also considered, with the width (b) varying between 20 and 40 cm, while the overall depth (h) varies between 20 and 80 cm. In all rectangular sections, $b/h = 2$ was adopted. This choice is justified by the fact that the rectangular cross-section is the most common in buildings. Typical values were adopted for the characteristic compressive strength of concrete (f_{ck}), opting for 30 and 60 MPa. Two ratios were considered for the first-order relative eccentricity (e_1/h), equal to 0.15 and 0.30. Furthermore, the geometric reinforcement ratio (ρ) was varied between 1.0 and 3.0%.

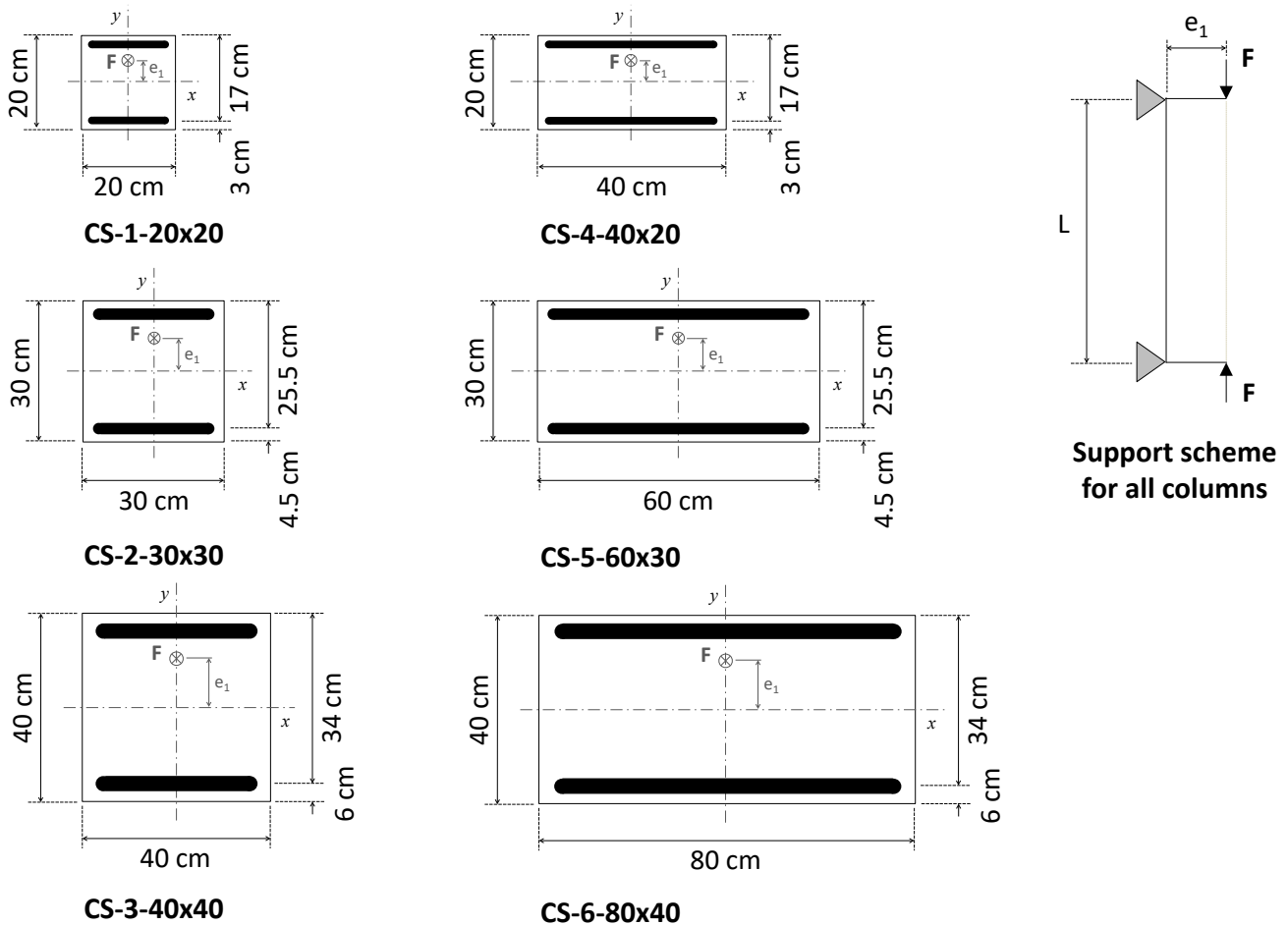


Figure 15 Cross-sections and support scheme for the columns considered in numerical tests.

All columns were considered subjected to sustained load. The effective creep coefficient $\varphi_{ef} = 1.18$ was applied, which concerns 75% of long-term loading, based on Casagrande (2016). This percentage corresponds to the usual condition for building projects. For steel properties, it was adopted the characteristic yield strength of reinforcement $f_{yk} = 500$ MPa and modulus of elasticity $E_s = 210$ GPa.

The forces and the respective resulting moments were determined by integrating the cross-section, divided into 20 strips. Concerning the calculation of the second-order effects, the equivalent cantilever column was considered divided into 10 sections. The moment-curvature diagram was made with an increment of the dimensionless curvature $\Delta\theta = 1$. The increment was reduced to $\Delta\theta = 0.1$, this being the ultimate curvature precision near the ultimate moment. The depth of the neutral line was determined to an accuracy of 1 mm. The values of the ultimate load were obtained in kN. All calculations were performed using computational tools implemented in object-oriented programming and spreadsheets. The algorithms were developed and implemented by the authors themselves. In this way, numerical tests could be performed on conventional computers.

The reliability index values obtained from the First Order Reliability Method (FORM) for the 432 tested columns are shown in Table 5.

Table 5 Reliability index (β) for very slender columns.

Cross-section	e_1/h	ρ (%)	$f_{ck} = 30$ MPa						$f_{ck} = 60$ MPa					
			Slenderness index (λ)						Slenderness index (λ)					
			100	120	140	160	180	200	100	120	140	160	180	200
CS-1-20x20	0.15	1.0	3.69	3.85	3.89	4.75	5.36	6.02	3.51	3.56	3.75	4.64	5.47	6.01
		2.0	3.37	3.32	3.36	4.13	5.01	5.44	3.25	3.26	3.34	4.24	4.92	5.60
		3.0	3.30	3.10	2.99	3.89	4.62	5.20	3.12	3.12	3.00	3.87	4.59	5.22
	0.30	1.0	3.31	3.36	3.35	4.18	4.79	5.48	3.32	3.35	3.30	4.09	4.94	5.67
		2.0	3.18	3.23	3.06	3.84	4.59	5.19	3.14	2.97	3.00	3.87	4.54	5.09
		3.0	3.30	3.07	3.07	3.80	4.51	4.94	3.05	3.05	2.87	3.70	4.41	5.02
CS-2-30x30	0.15	1.0	3.94	4.00	4.08	4.99	5.76	6.37	3.75	3.80	3.99	4.94	5.73	6.36
		2.0	3.46	3.44	3.49	4.33	5.07	5.70	3.39	3.42	3.44	4.35	5.10	5.75
		3.0	3.44	3.22	3.18	4.06	4.75	5.39	3.24	3.17	3.17	4.02	4.75	5.41
	0.30	1.0	3.44	3.54	3.49	4.35	4.97	5.62	3.50	3.39	3.43	4.25	5.08	5.79
		2.0	3.33	3.33	3.18	3.98	4.73	5.34	3.30	3.08	3.18	4.04	4.68	5.29
		3.0	3.46	3.15	3.20	4.00	4.65	5.20	3.20	3.19	3.01	3.87	4.59	5.23
CS-3-40x40	0.15	1.0	3.99	4.04	4.10	5.08	5.81	6.38	3.79	3.89	4.07	5.03	5.81	6.42
		2.0	3.51	3.48	3.53	4.40	5.14	5.78	3.45	3.43	3.51	4.39	5.15	5.82
		3.0	3.51	3.27	3.22	4.09	4.81	5.42	3.29	3.20	3.18	4.06	4.83	5.45
	0.30	1.0	3.48	3.58	3.54	4.35	5.03	5.67	3.51	3.50	3.45	4.32	5.09	5.88
		2.0	3.38	3.36	3.24	4.05	4.84	5.42	3.37	3.15	3.23	4.06	4.75	5.36
		3.0	3.49	3.21	3.24	4.02	4.70	5.27	3.25	3.22	3.07	3.90	4.66	5.29
CS-4-40x20	0.15	1.0	3.69	3.89	3.92	4.75	5.48	6.07	3.56	3.59	3.77	4.66	5.47	6.11
		2.0	3.36	3.38	3.37	4.22	4.95	5.54	3.27	3.24	3.31	4.15	4.90	5.57
		3.0	3.30	3.09	3.02	3.85	4.64	5.19	3.12	3.03	3.03	3.90	4.63	5.19
	0.30	1.0	3.34	3.45	3.34	4.16	4.89	5.35	3.32	3.32	3.30	4.16	4.93	5.66
		2.0	3.18	3.16	3.04	3.81	4.52	5.17	3.16	2.97	3.05	3.89	4.56	5.10
		3.0	3.38	3.05	3.01	3.76	4.45	4.98	3.05	3.06	2.88	3.72	4.41	5.02
CS-5-60x30	0.15	1.0	3.94	4.02	4.07	5.00	5.72	6.32	3.72	3.82	3.98	4.88	5.69	6.36
		2.0	3.48	3.42	3.47	4.32	5.06	5.70	3.38	3.41	3.46	4.37	5.12	5.75
		3.0	3.47	3.23	3.21	4.05	4.78	5.36	3.23	3.17	3.13	3.99	4.77	5.39
	0.30	1.0	3.45	3.51	3.50	4.32	4.99	5.63	3.51	3.44	3.42	4.28	5.07	5.81
		2.0	3.35	3.32	3.20	3.99	4.74	5.32	3.31	3.10	3.17	4.03	4.70	5.28
		3.0	3.48	3.16	3.18	3.98	4.62	5.16	3.23	3.16	3.05	3.86	4.62	5.19
CS-6-80x40	0.15	1.0	3.96	4.10	4.14	5.11	5.83	6.39	3.79	3.94	4.04	5.02	5.81	6.44
		2.0	3.49	3.49	3.53	4.40	5.16	5.77	3.42	3.47	3.50	4.38	5.15	5.84
		3.0	3.47	3.28	3.23	4.06	4.80	5.42	3.28	3.22	3.17	4.06	4.83	5.49
	0.30	1.0	3.51	3.56	3.54	4.36	5.04	5.67	3.51	3.45	3.45	4.33	5.10	5.85
		2.0	3.40	3.38	3.27	4.04	4.82	5.42	3.35	3.18	3.25	4.05	4.74	5.35
		3.0	3.50	3.20	3.22	3.99	4.71	5.27	3.24	3.23	3.10	3.90	4.69	5.28

6 RESULTS ANALYSIS

Based on the results obtained for the reliability index, an analysis of the structural safety of the elements was carried out. The following parameters were analyzed: cross-sections dimensions, compressive concrete strength, first-order relative eccentricity, slenderness index, and reinforcement ratio.

Through graphs, a visualization of the structural behavior is presented as the values of the variables undergo some change. To aid in the analysis, both the γ_{n1} application zone and the value of the target reliability index β_{target} were presented in most graphs. It is noteworthy that the additional coefficient γ_{n1} is defined by the Brazilian Standard NBR 6118 (ABNT, 2014) for columns with a slenderness index greater than 140, in the slenderness range in which only the

general method can be used. In turn, $\beta_{target} = 3.8$ was adopted based on Model Code 2010 (FIB, 2012). Finally, the probability of failure of the columns was evaluated.

6.1 Cross-section dimensions

Considering the division of the columns according to the type of cross-section, the results are grouped for 216 columns with a square section in Figure 16 and 216 columns with a rectangular cross-section in Figure 17.

It is observed that the dimensional variation influences the reliability index. In numerical tests, it is quite common to adopt a nominal standard deviation for both the width and the overall depth of the cross-section. Such adoption corresponds to minor errors in the formwork elaboration during the construction of bridges and buildings. Therefore, if the dimensions vary and the nominal error remains constant, it can result in a variation in reliability. The situation is worse for sections with a lower overall depth, as dimensional variation significantly reduces reliability.

Square and rectangular sections exhibit similar behavior. In both cases, the variation of the overall depth of the cross-section (h) should be noted. Cross-sections with $h = 20$ cm have a lower reliability index than the other cases. This indicates that sections of small overall depth should be avoided for greater safety of the structure. The Brazilian Standard NBR 6118 (ABNT, 2014) has an adjustment coefficient γ_n for sections with one dimension less than 19 cm. Therefore, an adjustment coefficient could be designed especially for very slender columns since even the dimension of 20 cm is inadequate in the safety analysis for $\lambda \leq 140$. Another way to solve this problem would be to implement an additional coefficient γ_{n1} that covers the entire range of elements with $90 < \lambda \leq 200$. It will be discussed below.

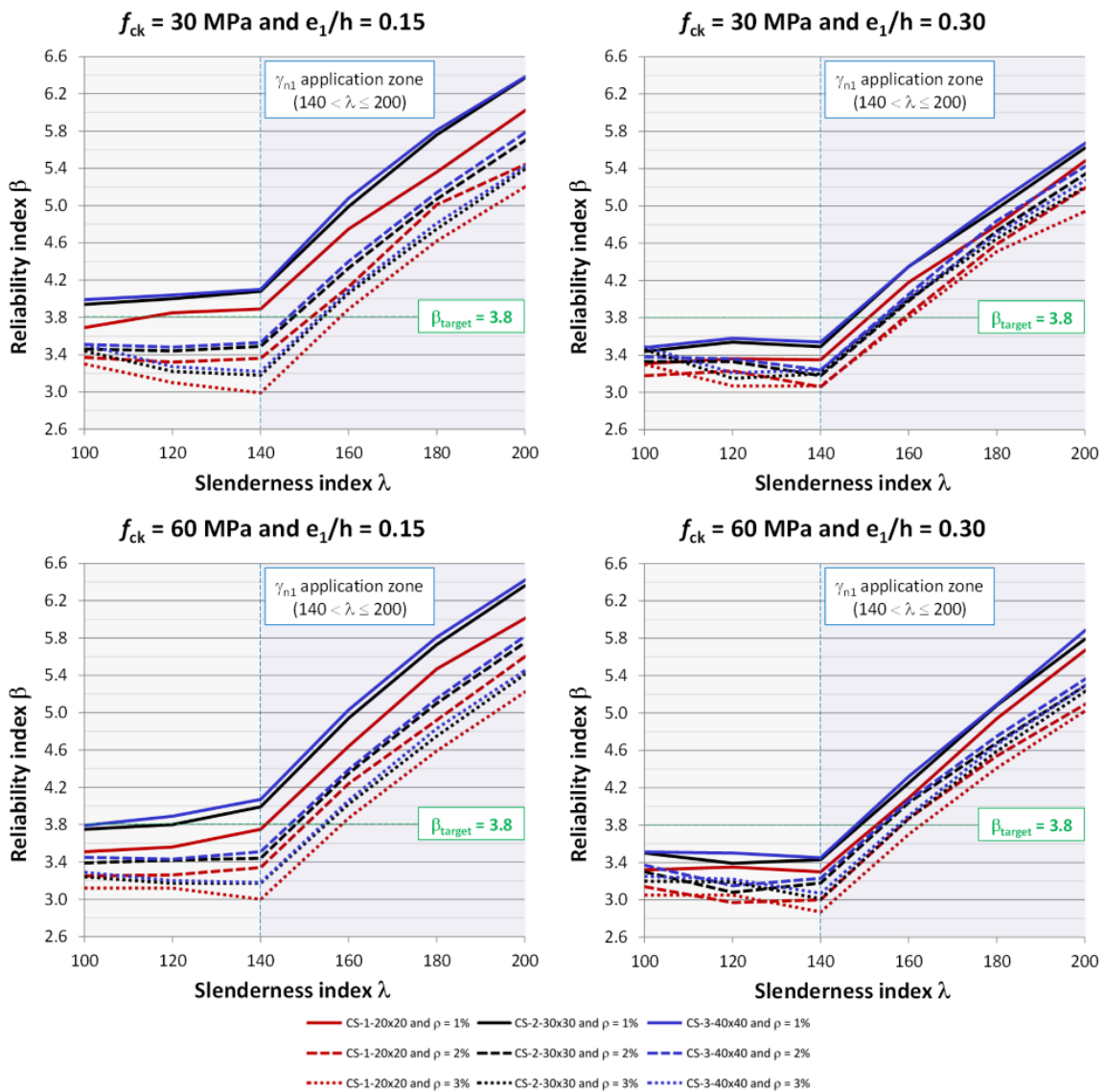


Figure 16 Analysis of the reliability index according to the dimensions of the square cross-section.

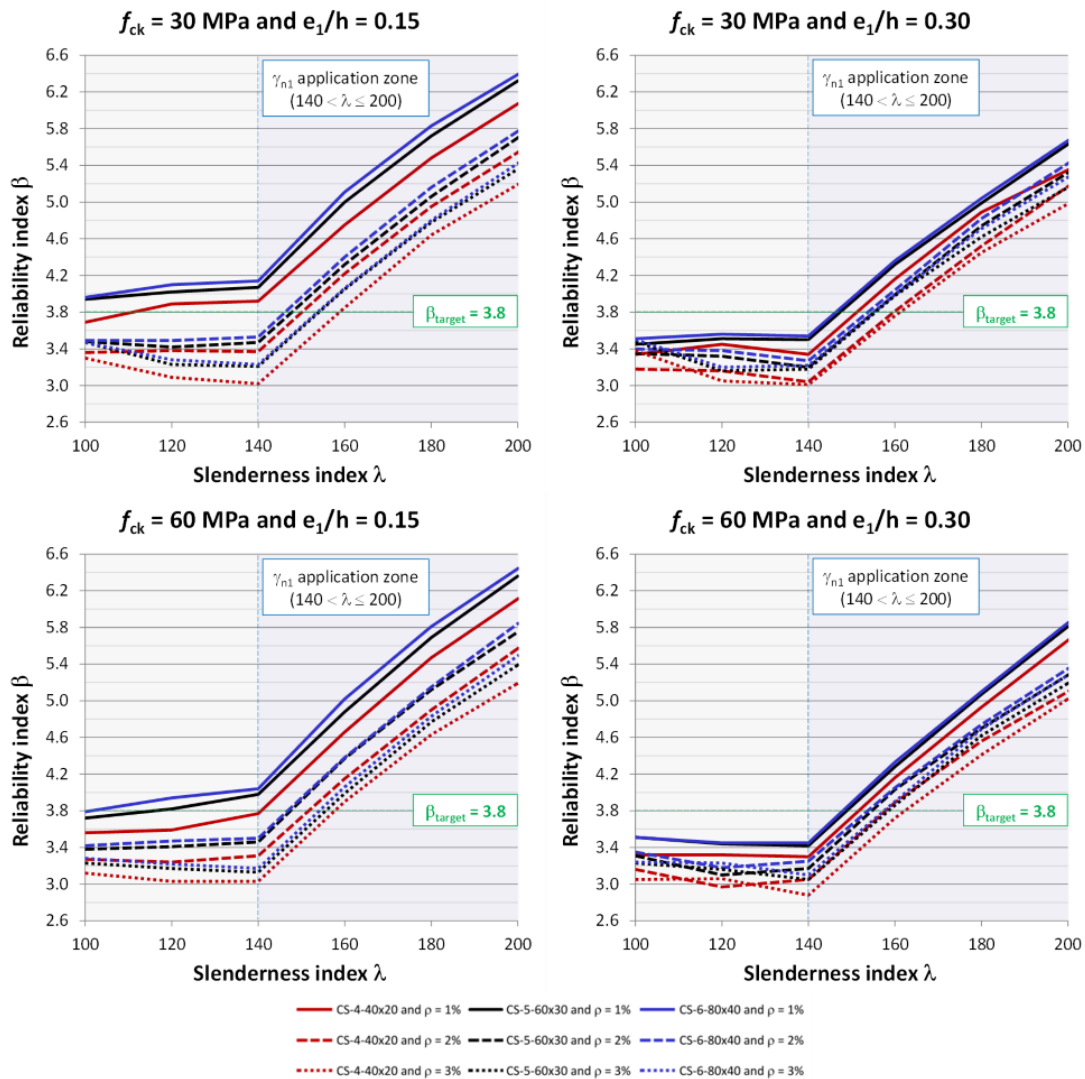


Figure 17 Analysis of the reliability index according to the dimensions of the rectangular cross-section.

6.2 Compressive concrete strength

As was done in the previous item, the columns were divided into two groups. The results obtained for the square section elements are shown in Figure 18 and for the rectangular section in Figure 19 concerning the variation of the compressive concrete strength.

In general, it is observed that it is not possible to state that there is any tendency to increase or decrease the reliability index when varying the characteristic compressive strength of concrete (f_{ck}). However, only two characteristic values were analyzed, $f_{ck} = 30$ MPa and $f_{ck} = 60$ MPa. Therefore, it is impossible to conclude that this is valid for the entire range of f_{ck} values, which varies between 20 and 90 MPa, according to Brazilian Standard NBR 6118 (ABNT, 2014). Because of this, it is intended to expand the analysis of the compressive concrete strength in future research.

6.3 First-order relative eccentricity

Bearing in mind that the eccentricity of an axial force produces a moment in the cross-section, and it influences the second-order effects, it is important to evaluate this variable. For this reason, the variation of the first-order relative eccentricity (e_1/h) was analyzed based on Figures 20 and 21. In numerical tests, $e_1/h = 0.15$ and $e_1/h = 0.30$ were adopted. This range includes many columns of buildings subjected to axial load and uniaxial bending moment.

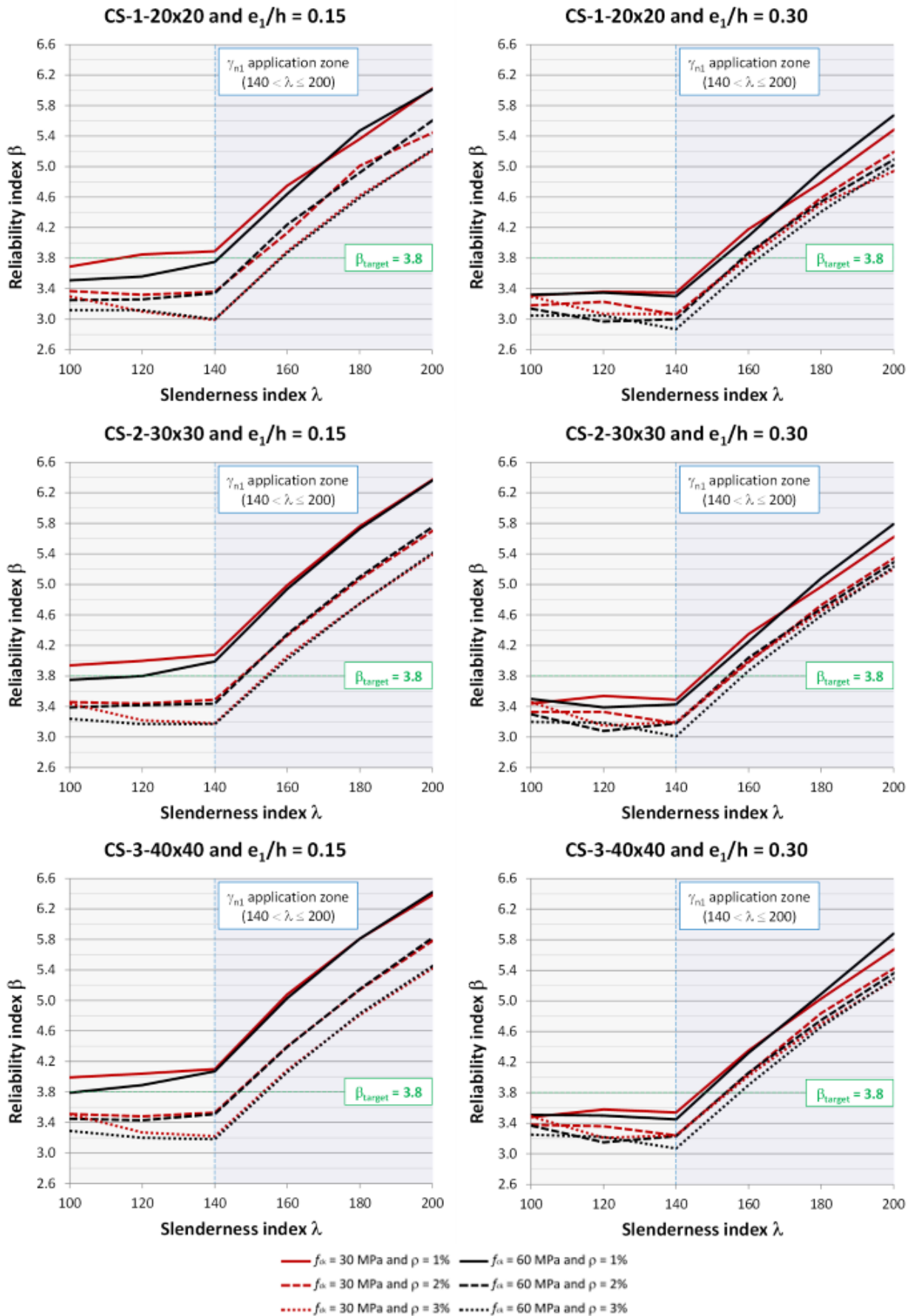


Figure 18 Analysis of the reliability index as a function of concrete strength for square cross-section.

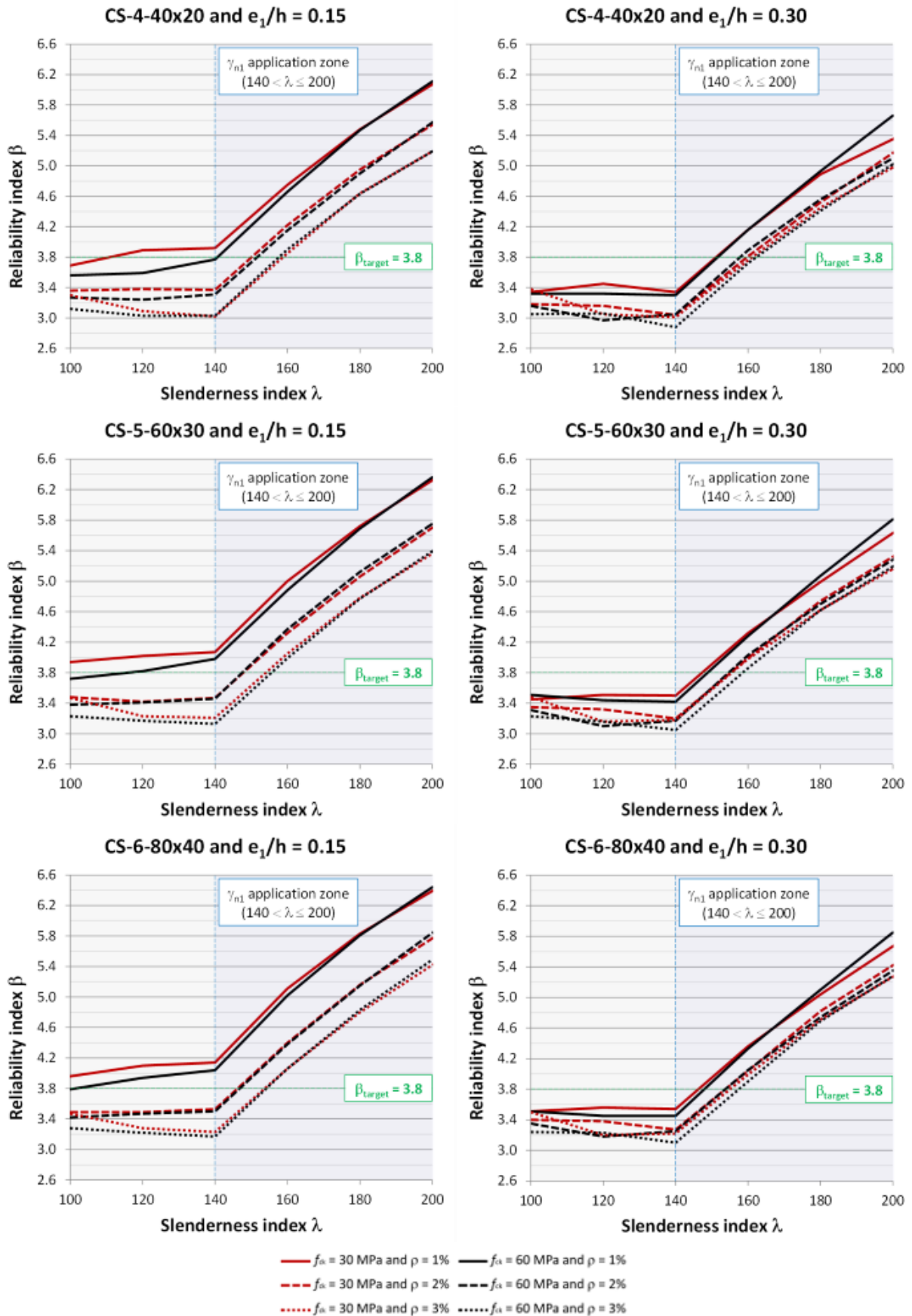


Figure 19 Analysis of the reliability index as a function of concrete strength for rectangular cross-section.

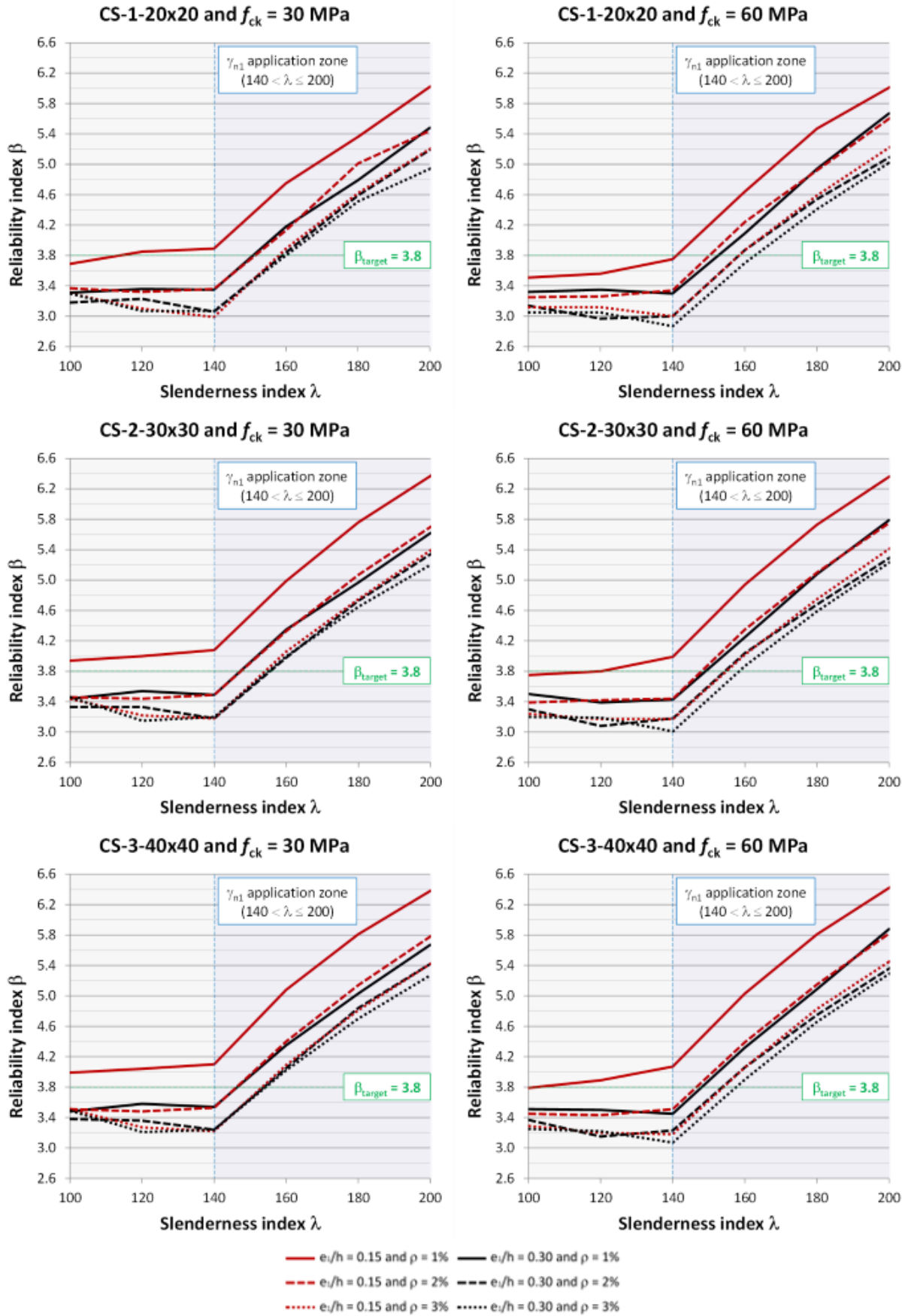


Figure 20 Analysis of the reliability index as a function of the relative eccentricity for square cross-section.

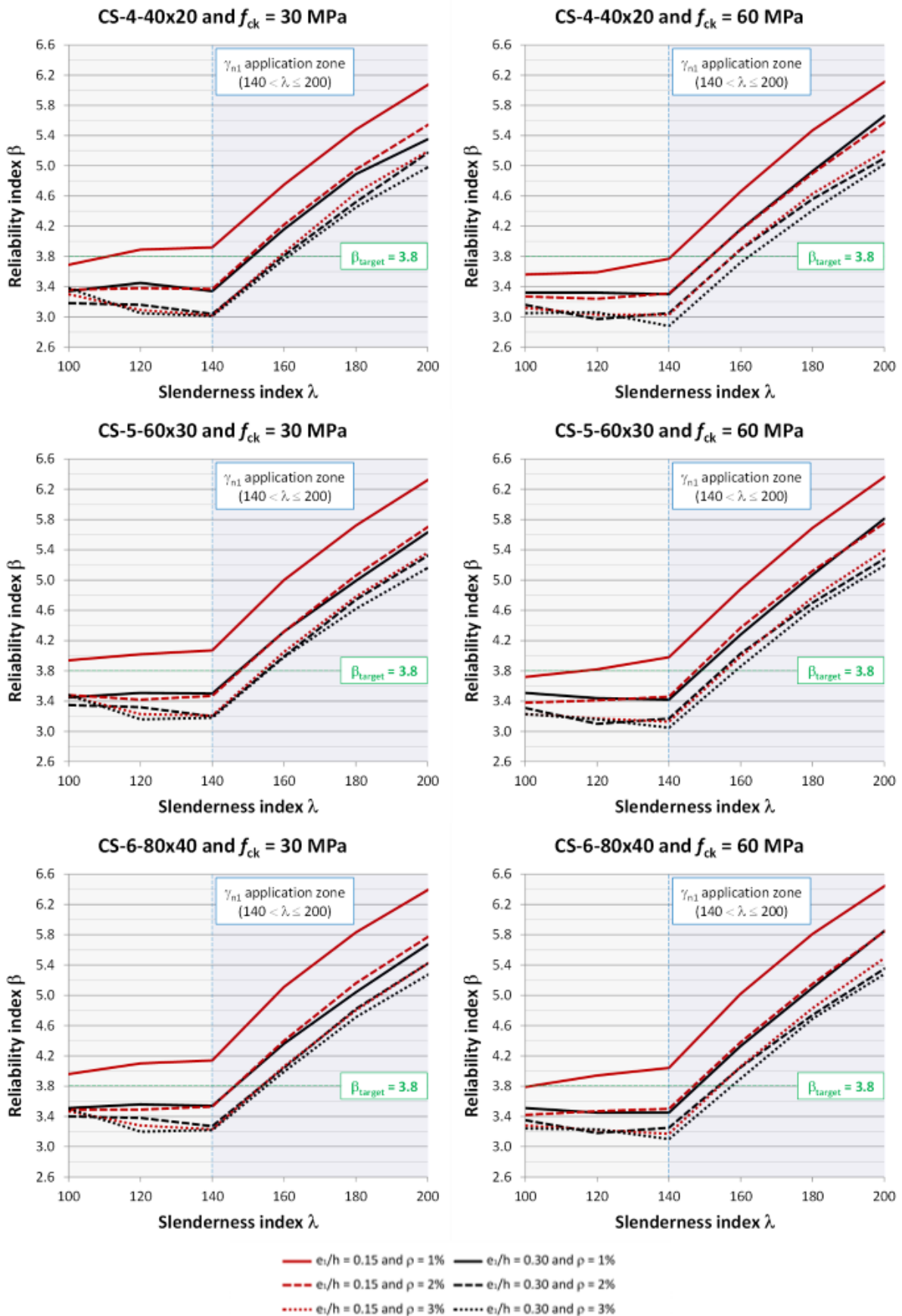


Figure 21 Analysis of the reliability index as a function of the relative eccentricity for rectangular cross-section.

For the elements with reinforcement ratio (ρ) of 1.0 and 2.0%, the superiority of the reliability index (β) was clear for lower first-order relative eccentricities. For $\rho = 3.0\%$, the curves became closer. Still, β is usually higher for $e_1/h = 0.15$ than for $e_1/h = 0.30$. This reduction of the reliability index with the increase in the relative eccentricity was also observed for columns with $\lambda \leq 90$, in Damas (2015), and Barbosa (2017).

6.4 Slenderness index

Typically, columns are evaluated for slenderness to determine which methods are allowed to calculate second-order effects. This parameter is also used to decide whether it is necessary to include the creep effect in the analysis. In parametric tests, the slenderness index between 100 and 200 was considered. The results obtained for the reliability index in function of the slenderness can be evaluated from Figures 16 to 21. However, to simplify the analysis, the values determined for the 432 columns were assembled in two scatter diagrams in Figure 22.

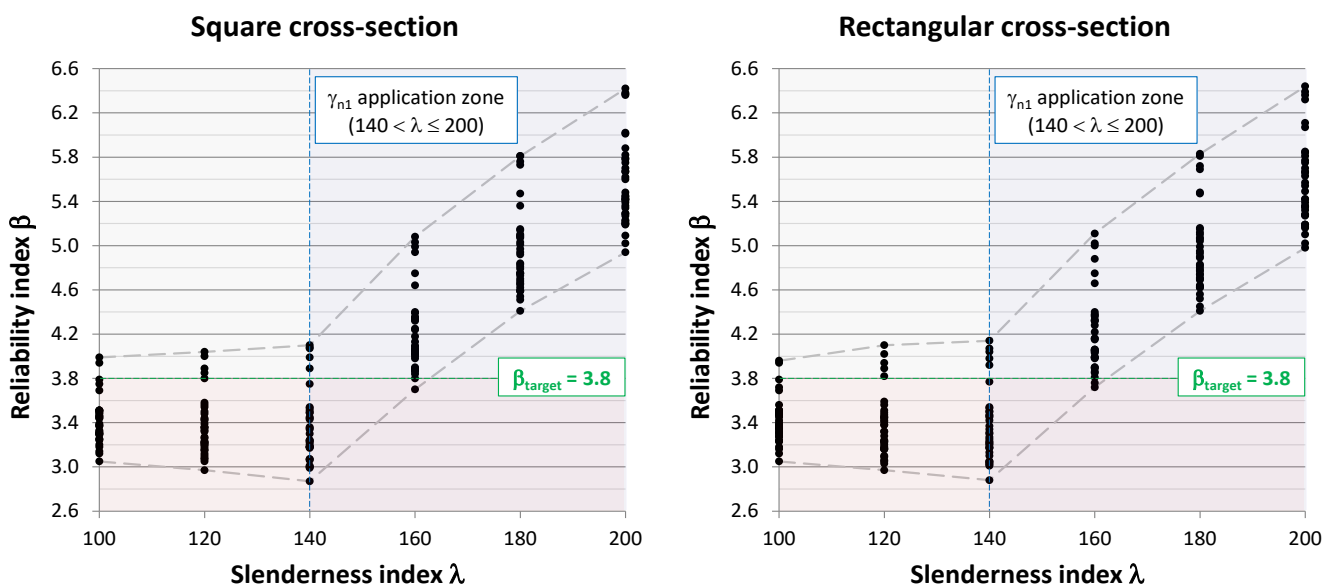


Figure 22 Analysis of the reliability index as a function of the slenderness index.

From Figure 22, it can be seen that the value of the reliability index β increases significantly to $\lambda > 140$. This is a practically linear increase. This is due to applying the additional coefficient γ_{n1} , adopted by the Brazilian Standard NBR 6118 (ABNT, 2014). In turn, for $\lambda \leq 140$, it is perceived that the current safety criterion is insufficient in several cases, as it results in reliability index values less than $\beta_{target} = 3.8$ and a significant probability of failure. Therefore, it is important to study the adoption of an additional safety factor for this slenderness range, covering all slender columns with $90 \leq \lambda \leq 200$. In addition, it is necessary to carry out the calibration of the additional coefficient to guarantee the safety of the structures without compromising the economy.

Although the other variables analyzed influence the value of the reliability index β , it is observed that most columns with $\lambda \leq 140$ has $\beta < \beta_{target}$. These results indicate a relationship between the slenderness index and the reliability of elements, regardless of the other factors. Therefore, an adequately adjusted additional coefficient γ_{n1} could solve this problem and circumvent the reduction in reliability promoted by other variables, such as cross-sections with reduced dimensions or with a high reinforcement ratio.

6.5 Reinforcement ratio

For the geometric reinforcement ratio (ρ) analysis, the format of the graphs was changed to visualize better the behavior of the columns as a function of this variable. As a result, all plotted curves are shown in Figure 23.

It is observed that the reliability index decreases when there is an increase in the reinforcement ratio, with some exceptions. However, such distinct behavior occurs only 14 times for this sample of 432 columns. Among all cases, the exception sometimes occurred for elements with $e_1/h = 0.30$, $\rho = 3.0\%$, and $\lambda \leq 140$, simultaneously.

Therefore, the increase in the reinforcement ratio ρ commonly causes a reduction in the reliability index β . This is due to the rise in the load capacity of the column. Under a more significant variable load, there is a greater effect caused by its coefficient of variation (COV), which has the highest COV among all random variables.

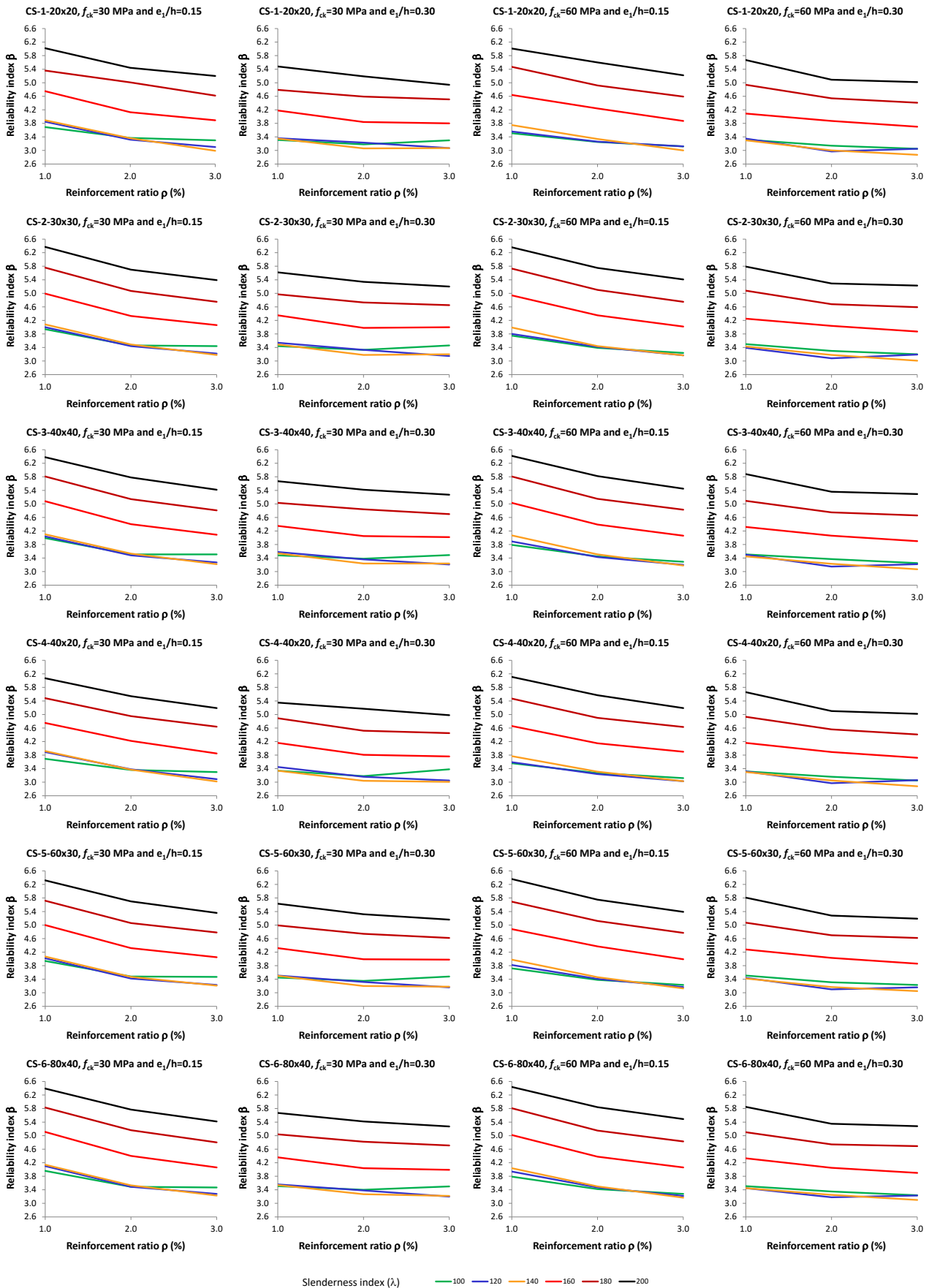


Figure 23 Analysis of the reliability index as a function of the reinforcement ratio.

6.6 Probability of failure

Another parameter used to analyze the risk of collapse of the structures is the probability of failure (P_f). As shown earlier, it can be determined from the reliability index (β). Their relationship is shown in Figures 24 and 25, for columns with slenderness index (λ) between 100 and 140 (within the range of $90 < \lambda \leq 140$ of the Brazilian Standard NBR 6118) and for columns with slenderness index between 160 and 200 (within the range of $140 < \lambda \leq 200$ and with the application of the additional coefficient γ_{n1}), respectively.

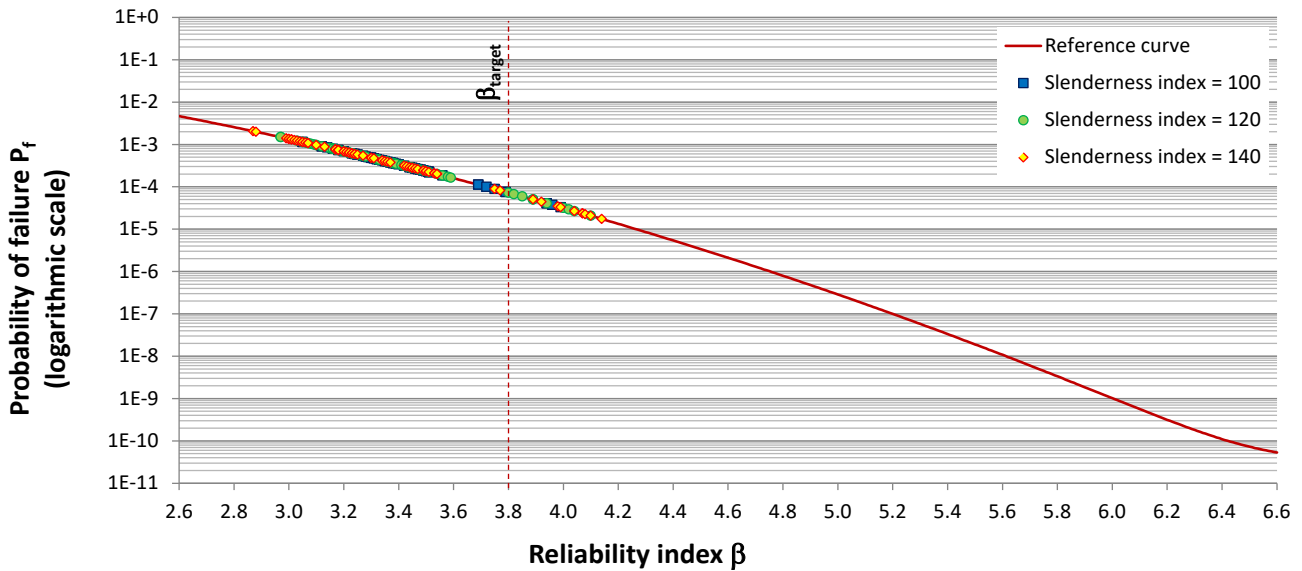


Figure 24 Probability of failure for columns with $90 < \lambda \leq 140$.

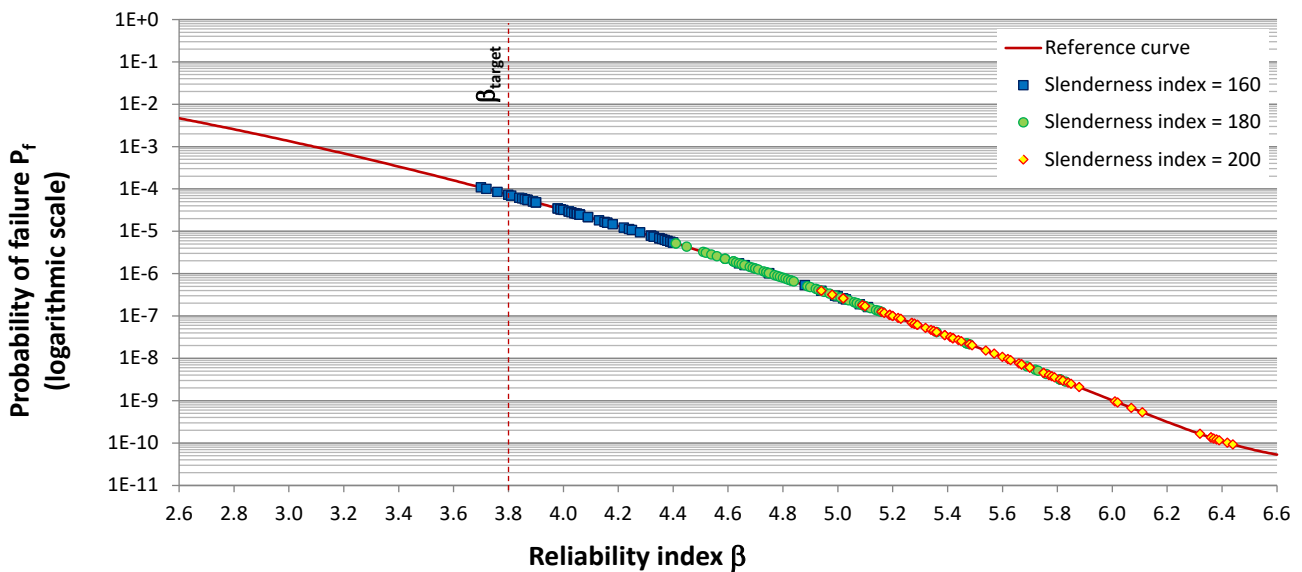


Figure 25 Probability of failure for columns with $140 < \lambda \leq 200$.

Commonly, the target reliability index $\beta_{target} = 3.8$ is adopted for reinforced concrete columns, based on Model Code 2010 (FIB, 2012). It is observed that the probability of failure for this value is 7.24×10^{-5} . However, its value must be evaluated according to the type of structure and the consequence of some structural failure. The probability of failure decreases exponentially as the value of the reliability index increases. This fact demonstrates the importance of adopting structural elements with a high reliability index to reduce the risk of structural collapse. The results show a higher risk for most elements with a slenderness index between 90 and 140. In contrast, elements with $140 < \lambda \leq 200$ have a reduced probability of failure due to the additional coefficient γ_{n1} .

7 CONCLUSION

The numerical tests showed that the general nonlinear method proves to be efficient for determining the ultimate load in very slender columns. However, it needs to be adjusted through an additional coefficient adequately calibrated to ensure structural safety. Based on the results obtained, the following conclusions are admitted:

- **elements with a small overall depth of the cross-section ($h = 20$ cm) have a lower reliability index than larger sections**, considering square cross-sections with dimensions ranging from 20 to 40 cm and rectangular cross-sections with the proportion $b = 2h$, denoting the need to implement a safety factor to cover this problem or limit the use of reduced sections on very slender columns;
- **elements with a square or rectangular cross-section have a similar reliability index**, as long as they have the same overall depth of the cross-section, considering the proportion $h = b$ with $20 \text{ cm} \leq h \leq 40 \text{ cm}$ for square cross-section and $b = 2h$ for rectangular cross-section in all tests performed;
- **the variation in the concrete strength did not significantly affect the value of the reliability index**, but this aspect needs to be better evaluated because only $f_{ck} = 30 \text{ MPa}$ and $f_{ck} = 60 \text{ MPa}$ were considered in numerical tests, within the range of 20 to 90 MPa allowed by the Brazilian Standard NBR 6118 (ABNT, 2014);
- **the increase in the first-order relative eccentricity reduces the reliability index**, having been considered $e_1/h = 0.15$ and $e_1/h = 0.30$ in the tests;
- **the design criteria for the columns with a slenderness index between 90 and 140 require adjustments**, since the target reliability index β_{target} in this range was not reached for most elements, adopting the general nonlinear method with the displacement of the stress-strain diagram due to creep;
- **the reliability of columns with slenderness index above 140 commonly exceeds the target reliability index**, adopting the additional coefficient γ_{n1} proposed by the Brazilian Standard NBR 6118 (ABNT, 2014) and considering $\beta_{\text{target}} = 3.8$, based on the Model Code 2010 (FIB, 2012);
- **the increase in the reinforcement ratio commonly reduces the reliability index**, except for specific cases, when varying e_1/h between 0.15 and 0.30, ρ between 1.0 and 3.0%, and λ between 100 and 200, since that only some columns with $e_1/h = 0.30$, $\rho = 3.0\%$ and $\lambda \leq 140$ were the exception to this proposition.

In summary, it is observed that the Brazilian Standard NBR 6118 (ABNT, 2014) was careful concerning the columns with $\lambda > 140$. The additional coefficient γ_{n1} corrects possible reductions in reliability index due to several factors: small dimensions of the cross-section, high longitudinal reinforcement ratio, high variation of the variable load, among other building design conditions. However, this coefficient requires calibration. Another point to be considered is that the application zone of the coefficient needs to be expanded, as the columns with $90 < \lambda \leq 140$ have a significant probability of failure in comparison with other slenderness ranges.

Taking into account that this research integrates a more comprehensive program about the reliability of very slender columns, it is intended to develop a proposal for an additional safety factor for $90 < \lambda \leq 200$ in future works. In this way, it is intended to contribute to the knowledge about the highly slender columns and provide a basis for future normative revisions.

Acknowledgements

The author K. Ribeiro thanks the Universidade Federal de Santa Catarina (UFSC), the Coordenação de Aperfeiçoamento de Pessoal de Nível Superior (Capes), and the Universidade do Estado de Santa Catarina (UDESC). The author M. de V. Real thanks the Conselho Nacional de Desenvolvimento Científico e Tecnológico (CNPq) for the research grant (Process 304211/2018-4).

Author's Contributions: Conceptualization, K Ribeiro, DD Loriggio, M de Vasconcellos Real; Data curation, K Ribeiro; Formal Analysis, K Ribeiro; Investigation, K Ribeiro; Methodology, K Ribeiro, DD Loriggio, M de Vasconcellos Real; Software, K Ribeiro; Supervision, DD Loriggio, M de Vasconcellos Real; Validation, K Ribeiro; Writing – original draft, K Ribeiro; Writing – review & editing, K Ribeiro, DD Loriggio, M de Vasconcellos Real.

Editor: Marcílio Alves.

References

- ABNT (2014). NBR 6118:2014. Projeto de estruturas de concreto – Procedimento. Rio de Janeiro, Brazil.
- Barbosa, P. R. O. (2017). Análise probabilística de pilares de concreto armado através do método dos elementos finitos, M.S. thesis (in Portuguese), PPGEC, UFRGS, Porto Alegre, Brazil.
- Benko, V., Dobrý, J., Čuhák, M. (2019). Failure of slender concrete columns due to a loss of stability, *Slovak Journal of Civil Engineering*, vol. 27, no. 1, pp. 45-51, Apr 2019 (Published Online), <https://doi.org/10.2478/sjce-2019-0007>.
- Casagrande, A. F. (2016). Consideração da fluência no cálculo dos efeitos de segunda ordem em pilares de concreto armado, M.S. thesis (in Portuguese), PPGEC, UFSC, Florianópolis, Brazil.
- CEN (2004). EN 1992-1-1:2004. Eurocode 2: Design of concrete structures - Part 1-1: General rules and rules for buildings. Brussels, Belgium.
- Claeson, C., Gylltoft, K. (1998). Slender high-strength concrete columns subjected to eccentric loading, *J Struct Eng*, vol. 124, pp. 233–240, Mar. 1998, [https://doi.org/10.1061/\(ASCE\)0733-9445\(1998\)124:3\(233\)](https://doi.org/10.1061/(ASCE)0733-9445(1998)124:3(233)).
- Collins, M. P., Mitchell, D. (1997). *Prestressed concrete structures*, Toronto, Canada, Response Publications.
- Damas, A. P. (2015). Estudo de confiabilidade no projeto de pilares esbeltos de concreto de alta resistência, M.S. thesis (in Portuguese), PPGEC, UFRGS, Porto Alegre, Brazil.
- Dantas, A. B. (2006). Estudo de pilares de concreto armado submetidos à flexão composta reta, M.S. thesis (in Portuguese), PECC, UnB, Brasília, Brazil.
- Enciso, R. O. (2010). Comportamento de pilares esbeltos de concreto de alta resistência sujeitos à flexão composta reta, M.S. thesis (in Portuguese), PPGEC, PUC-Rio, Rio de Janeiro, Brazil.
- FIB (2012). Model Code 2010: Final draft, Bulletin 65, Vol. 1, Lausanne, Switzerland.
- Fusco, P. B. (1981). *Estruturas de concreto: solicitações normais*. Rio de Janeiro, Brazil, Guanabara Dois.
- Goyal, B. B., Jackson, N. (1971). Slender concrete columns under sustained load, *J Struct Div*, vol. 97, no. 11, pp. 2729–2750, Nov. 1971, <https://doi.org/10.1061/JSDEAG.0003050>.
- Khalil, N., Cusens, A. R., Parker, M. D. (2001). Tests on slender reinforced concrete columns. *The Structural Engineer*, vol. 79, no. 18, Sept. 2001.
- Kim, J.-K., Lee, S.-S. (2000). The behavior of reinforced concrete columns subjected to axial force and biaxial bending, *Engng Struct*, vol. 22, no. 11, pp. 1518–1528, Nov. 2000, [https://doi.org/10.1016/S0141-0296\(99\)00090-5](https://doi.org/10.1016/S0141-0296(99)00090-5).
- Kim, J.-K., Yang, J.-K. (1995). Buckling behaviour of slender high-strength concrete columns, *Engng Struct*, vol. 17, no. 1, pp. 39–51, 1995, [https://doi.org/10.1016/0141-0296\(95\)91039-4](https://doi.org/10.1016/0141-0296(95)91039-4).
- Klein Júnior, O., Stucchi, F. R., Barbosa, R. L. (2020). Evaluation of Brazilian standard ABNT NBR 6118 procedures for calculating the second-order effects of reinforced concrete slender columns subjected to uniaxial bending, *Structural Concrete*, vol. 21, no. 1, pp. 81-93, Feb. 2020, <https://doi.org/10.1002/suco.201800251>.
- Kordina, K. (1972). *Langzeitversuche an stahlbetonstützen*, Institut für Baustoffkunde und Stahlbetonbau, Technische Universität Braunschweig, Braunschweig, June 1972.
- Magalhães, F. C. (2014). A problemática dos concretos não conformes e sua influência na confiabilidade de pilares de concreto armado, Ph.D. thesis (in Portuguese), PPGEC, UFRGS, Porto Alegre, Brazil.
- Magalhães, F. C., de Vasconcellos Real, M., da Silva Filho, L. C. P. (2016). The problem of non-compliant concrete and its influence on the reliability of reinforced concrete columns, *Mater Struct*, vol. 49, pp. 1485-1497, <https://doi.org/10.1617/s11527-015-0590-x>.
- Melo, C. E. L. de. (2009). Análise experimental e numérica de pilares birrotulados de concreto armado submetidos a flexo-compressão normal, Ph.D. thesis (in Portuguese), PECC, UnB, Brasília, Brazil.
- Mirza, S. A., Skrabek, B.W. (1991). Reliability of short composite beam-column strength interaction, *J. Struct. Eng.*, vol. 117, no. 8, pp. 2320-2339, Aug. 1991, [https://doi.org/10.1061/\(ASCE\)0733-9445\(1991\)117:8\(2320\)](https://doi.org/10.1061/(ASCE)0733-9445(1991)117:8(2320)).

Nogueira, H. A. T. (2006). Avaliação da confiabilidade de pilares curtos em concreto armado projetados segundo a NBR 6118:2003, M.S. thesis (in Portuguese), UFMG, Belo Horizonte, Brazil.

Nowak, A. S., Collins, K. R. (2000). Reliability of structures, McGraw-Hill.

Ramu, P., Grenacher, M., Baumann, M., Thürlimann, B. (1969). Versuche an gelenkig gelagerten Stahlbetonstützen unter Dauerlast, Institut für Baustatik, Eidgenössische Technische Hochschule Zürich, Zürich, 1969, <https://doi.org/10.3929/ethz-a-004170564>.

Santiago, W. C., Kroetz, H. M., Santos, S. H. C., Stucchi, F. R., Beck, A. T. (2020). Reliability-based calibration of main Brazilian structural design codes, Latin American Journal of Solids and Structures, vol. 17, no. 1, Dec. 2019 (available online), <https://doi.org/10.1590/1679-78255754>.

Strauss, A., Zimmermann, T., Spyridis, P., Täubling, B. (2018). Bearing capacity of slender concrete columns, Slovak Journal of Civil Engineering, vol. 26, no. 4, pp. 39-49, Jan. 2019 (Published Online), <https://doi.org/10.2478/sjce-2018-0027>.

Westerberg, B. (2008). Time-dependent effects in the analysis and design of slender concrete compression members, Ph.D. thesis, Division of Concrete Structures, Stockholm, Sweden.